Black Holes: New Perspectives from Higher Dimensions

Nidal Haddad

Black Holes: New Perspectives from Higher Dimensions

Memòria presentada per a optar al títol de Doctor en Física per

Nidal Haddad

Departament de Física Fonamental i
Institut de Ciències del Cosmos, Universitat de Barcelona,
Martí i Franquès 1, E-08028 Barcelona

Programa de doctorat de Física
Universitat de Barcelona

Dirigida pel Prof. **Roberto Emparan**

To my parents

Contents

Acknowledgements

I would like to thank Roberto Emparan for supervising me throughout the four years of the PhD period, for teaching me, and for letting me work on interesting and diverse problems. I would like to thank also the members of our group, the "Gravitation and Cosmology Group" of the university of Barcelona, Enric Verdaguer, Jaume Garriga, David Mateos, and Bartomeu Fiol.

It was a pleasure and of great help during my PhD period to have been friends, and office mates at the same time, with Guillem Perez, Nico geisel, Martin Goethe, Maria Aznar, and Markus Frob. It was a pleasure as well to have Sudipto Muhuri and Paolo Indescai as friends. I would like to thank Joan Camps for both friendship and collaboration. Special thanks are for my friend Hicham Bakkali for excellent times and encouragement.

Finally, I would like to thank my parents, Fateen and Ahlam, for their very generous support, for their full trust in me, and for their permanent encouragment during my PhD period, without whom I would not have been able to reach this stage. The same is true for my family as a whole, my parents, my beloved little sister, Fatima Al-Zahraa, my brother (and friend) Alaa and his wife Donia.

Chapter 1

Resum en català

Malgrat el seu èxit a nivell clàssic, la relativitat general s'enfronta a problemes de no-renormalitzabilitat a nivell quàntic. No obstant, prediu l'existència de forats negres, que són objectes tèrmics que s'espera que continuin existint en una teoria satisfactòria de gravetat quàntica. La seva consistència matemàtica requereix que l'espai-temps tingui deu dimensions, i d'aquesta manera motiva l'estudi de la relativitat general, i en particular els forats negres, en dimensions altes. Aquest és el tema central de la nostra tesi. A més, l'adveniment de la correspondència AdS/CFT, que relaciona una teoria de gravetat amb una teoria quàntica de camps en una dimensió menys, ha incrementat encara més l'interès en la gravetat en dimensions altes. Comparada amb la relativitat general en quatre dimensions, que ha estat àmpliament estudiada i investigada els darrers anys, la relativitat general en dimensions més altes té moltes característiques noves i interessants.

La unicitat és una propietat de la relativitat general en quatre dimensions que no continua sent vàlida en dimensions més altes. Una altra propietat relacionada amb aquesta és que en quatre dimensions els forats negres només poden tenir horitzons amb topologia esfèrica, mentre que en dimensions més altes els objectes negres poden tenir també altres topologies. Els anells negres són una manifestació d'això. Les dues noves propietats esmentades donen lloc a transicions de fase topològiques a l'espai de fases dels forats negres en dimensions altes, que és un dels temes que considerem i als quals contribuim en aquesta tesi.

L'existència d'objectes negres estesos en dimensions altes, anomenats p-branes negres, és un tema important i fonamental. Se sap que aquests objectes són dinàmicament inestables. Per tant, la qüestió de cap on condueix aquesta inestabilitat ha esdevingut un problema important. Quin és l'estat final? Aquesta inestabilitat es coneix com la inestabilitat de Gregory-Laflamme i és un altre tema que investiguem a la nostra tesi, i que relacionem amb un tipus de correspondència entre fluids i gravetat a l'espai-temps

pla. L'existència de p-branes negres s'atribueix al fet que en relativitat general en dimensions altes hi ha forats negres que poden rotar de manera arbitràriament ràpida. És a dir, no hi ha un anàleg de la cota de Kerr en quatre dimensions, que impedeix que els forats negres donin voltes molt de pressa. La rotació ràpida, per altra banda, que és possible en dimensions més altes té l'efecte d'aplanar l'horitzó del forat negre al llarg del pla de rotació, i per tant en el limit de velocitats altes s'aproxa a la geometria de la p-brana negra.

Al capítol 3 donem una breu introducció a l'estudi de forats negres en dimensions més altes per mitjà de les anomenades "blackfolds". Discutim les raons per les quals hom pot fer servir nous mètodes aproximats en dimensions més altes. Introduim els objectes bàsics de l'enfoc amb blackfolds, les p-branes negres impulsades, i expliquem com l'enfoc amb blackfolds es pot fer servir per construir a partir d'elles noves solucions estacionàries de les equacions del camp gravitatori amb noves topologies, i com es pot fer servir també per construir solucions dinàmiques.

Al capítol 4 donem una breu introducció al tema dels canvis de topologia en relativitat general. Discutim les fases del forat negre de Kaluza-Klein, la fase de corda negra homogènia, la fase de corda negra inhomogènia i fase de forat negre localitzat. Expliquem el mecanisme pel qual apareix una transició de fase topològica quan hom es mou per l'espai de fases des d'una corda negra fins a un forat negre localitzat.

Al capítol 5 hem aconseguit formular un tipus de correspondència entre fluids i gravetat a l'espai pla. Hem trobat un mapa entre una p-brana negra impulsada fluctuant i un fluid viscós relativista situat a l'infinit espacial. És a dir, hem construit una solució de les equacions d'Einstein al buit d'una p-brana negra dinàmica fins a primer ordre en derivades. El fluid viscós dual està caracteritzat per dos paràmetres (coeficients de transport) al tensor d'energia-moment, la viscositat de cisallament i la viscositat de compressió. Fent servir la solució gravitatòria hem pogut calcular aquests coeficients. A saber, hem trobat que el tensor d'energia-moment del fluid és

$$T_{ab} = \rho u_a u_b + P P_{ab} - \zeta \theta P_{ab} - 2\eta \sigma_{ab} + O(\partial^2) \tag{1.0.1}$$

on

$$\eta = \frac{\Omega_{n+1}}{16\pi G} r_0^{n+1} \,, \qquad \zeta = \frac{\Omega_{n+1}}{8\pi G} r_0^{n+1} \left(\frac{1}{p} + \frac{1}{n+1} \right) \,. \tag{1.0.2}$$

són les viscositats de cisallament i de compressió respectivament. A dalt, totes les quantitats termodinàmiques estan donades en termes del radi de Schwarzschild de la brana negra, r_0. A més, fent servir la descripció efectiva de la p-brana negra com un fluid viscós en un nombre més baix de dimensions hem estudiat la inestabilitat de Gregory-Laflamme, i els nostres resultats estan d'acord de manera molt precisa amb els resultats numèrics prèviament obtinguts en aquest problema (que havien estat

obtinguts per mitjà d'una anàlisi de les equacions gravitatòries linealitzades). Més en detall, incloent l'efecte d'amortiment de la viscositat en les ones de so inestables hem obtingut una aproximació remarcablement bona i senzilla a la relació de dispersió dels modes de Gregory-Laflamme, la precisió de la qual augmenta amb el nombre de dimensions transverses. Hem proposat una forma límit exacta quan el nombre de dimensions tendeix a infinit. Així, en lloc d'intentar resoldre les complicades equacions gravitatòries (linealitzades) proposem intentar resoldre les equacions relativistes de Navier-Stokes per al fluid efectiu (dual), ja que aquestes són molt més senzilles que les primeres.

Al capítol 6 hem abordat i hem fet progrés en un altre problema: canvi de topologia en relativitat general en dimensions més altes. Abans del nostre treball no hi havia cap exemple analític complet (només n'hi havia de numèrics) d'una transició de fase topològica en relativitat general. La transició de fase corda negra/ forat negre en espais de Kaluza-Klein havia estat analitzada i estudiada només numèricament. No obstant, alguns models locals havien estat obtinguts analíticament. S'havia argumentat que la transició de fase passa (o és mediada) per una configuració crítica singular: una geometria de doble con autosimilar. Aquesta geometria s'havia trobat **només localment**, però. Al nostre treball hem proporcionat per primera vegada un exemple analític complet d'una transició de fase topològica. Hem considerat el forat negre en rotació dins l'espai de de-Sitter (el forat negre de Kerr-de-Sitter), i hem mostrat que si hom segueix una trajectòria a l'espai de fases al llarg de la qual la rotació del forat negre augmenta llavors aquest s'aplanarà i estirarà al llarg del pla de rotació, i finalment tocarà l'horitzó de de-Sitter allà on aquest horitzó s'intersecta amb el pla de rotació. S'obté una transició de fusió si hom continua movent-se al llarg de la mateixa trajectòria a l'espai de fases, després de la qual s'arriba a a una fase fusionada amb un únic horitzó connectat. Al nostre exemple, la configuració crítica (en la qual els dos horitzons es troben) és mediada per un doble con autosimilar, la qual cosa confirma propostes prèvies quant al mecanisme pel qual funcionen les transicions de fase topològiques.

També hem descrit models locals per a les geometries crítiques que controlen moltes transicions a l'espai de fases de forats negres en dimensions més altes, tals com la transició d'un forat negre topològicament esfèric a un anell negre o a una p-esfera negra, o la fusió de forats negres i anells negres en Saturns negres o di-anells en $D \geq 6$.

Val la pena esmentar, a més, que els cons que hem trobat són generals (comparats amb els coneguts prèviament) en el sentit que descriuen dos horitzons que s'intersecten a temperatures que poden diferir. No obstant, en el cas en què els dos horitzons s'intersecten a a temperatures diferents no hi pot haver una transició de fusió posteri-

orment, i per tant la trajectòria de solucions a l'espai de fases s'acaba allà.

Chapter 2

Introduction

2.1   General relativity in 4 dimensions

However successful general relativity is when one uses it to describe classical phenomena concerning the gravitational force [1, 2, 3], it goes bad when one tries to quantize it and to use it to describe quantum phenomena. Not so bad though; surprisingly, on the classical level it predicts the presence of some objects, called black holes, which, based on a semi-classical treatment, turn to posses all properties to qualify as thermal objects. A temperature and entropy were associated to these objects [4, 5] and they were shown to satisfy the laws of thermodynamics. The surprise lies in the fact that the thermodynamic properties of black holes, which one is supposed to read from the quantum theory, were found based on a semi-classical theory of general relativity, known as Hawking radiation [5].

Therefore, even though general relativity in 4 dimensions is a non-renormalizable field theory − in fact, that is true also for any number of dimensions larger than 4 − it can be still trusted at the semi-classical level, that is, when one studies quantum fields on curved and fixed classical backgrounds [6]. So that, even in a satisfactory theory of quantum gravity it is expected that some aspects of general relativity, modified slightly most probably, will remain, such as black holes.

One fascinating and puzzling feature of black holes is that their entropy is given (in gravitational units) by 1/4 of the area of the event horizon, which is the Bekenstein-Hawking entropy formula [4, 5]. Whereas for field theories, in general, the entropy is proportional to the volume of the system, for black holes it is proportional to the area. This implies, somehow, that black hole physics is holographic [7, 8] − the information of the inside of a black hole, inside its three-dimensional volume, is stored on its boundary, a two-dimensional surface.

Uniqueness is one of some features special to 4 dimensional general relativity [9].

In Einstein-Maxwell's theory, given certain values of mass, angular momentum, and charge, there is only one black hole with such a set of values, namely, the charged Kerr black hole. Of course, the property that black holes are characterized by 3 parameters only, in the Einstein-Maxwell theory for example, for whatever initial data the space-time contained before their formation, is known as the "no hair" property of black holes [9]. Another feature of black holes special to 4 dimensions is that their horizons must have spherical topology. There are no black hole solutions with a different topology in 4 dimensions.

The Kerr-bound is one more special character of 4 dimensional general relativity. The speed of rotation of a rotating black hole is bounded from above. In other words, in 4 dimensions black holes can not rotate very fast.

2.2   String theory predicts extra dimensions

String theory provides one of the most successful approaches, today, to reconcile and unify gravity and quantum mechanics [10, 11]. String theory basic assumption is that the fundamental object in nature is not a point-like object, but rather a one-dimansional object, with zero thickness − a string. Upon quantizing the string one recognizes the different oscillation modes (or quantum states) of the string with different particles. In special, it gives rise to a massless, spin-two particle, the graviton.

General relativity is naturally incorporated in string theory. It gets modified at very short distances / high energies, but at ordinary distances and energies it is present in exactly the same form as proposed by Einstein. The importance of this is that general relativity arises within the framework of a consistent quantum theory.

To obtain a realistic and consistent string theory one must require supersymmetry as well, and hence the name superstring theory. Superstring theories are able to predict the dimension of spacetime in which they live. The theories are consistent in 10 dimensions and in some cases (M-theory) an eleventh dimension is also possible. To make contact between string theory and the four-dimensional world of everyday experiences, the most straightforward possibility is that six or seven of the dimensions are compactified on an internal manifold, whose size is sufficiently small to escape detection. This reminds us of the Kaluza-Klein theory, which is an attempt to unify gravity and electromagnetism by compactifing five-dimensional general relativity on a circle. String theory has many analogous compactifications. It is important to mention that even if the internal manifolds are invisible at long distances or low energies their topological properties determine the particle content and structure of the four-dimensional theory.

As for black holes that come from string theory, it is worth saying that one of the

most striking successes of string theory so far is the counting of microstates of certain black holes [12] and, consequentely, the derivation of the Bekenstein-Hawking entropy formula. The last counting, however, is more successful when there is a large amount of supersymmetry. This correct counting using the microscopic degrees of freedom of string theory, in this case what are known as $D-$branes, gathers a lot of evidence that string theory is a theory of quantum-gravity.

As a result, one concludes that to make contact with string theory one should be working with general relativity in higher dimensions (compactified or not) and so, before all, one should be able to tell / know the differences between 4 and higher dimensional gravity. As we are going to mention next, higher dimensional general relativity differs from its four-dimensional counter part in many significant aspects.

2.3   Black holes in higher dimensions

As explained above, string theory motivates and shows the importance of the study of higher dimensional general relativity. In special, it motivates the study of its basic obects, i.e., higher dimensional black holes. Even though black holes that come from string theory are, generically, charged objects, to understand the new phenomena and differences that arise in higher dimensions, compared to 4 dimensions, it is wise to start first by studing neutral black holes, being the simplest cases.

We start by the observation that in higher dimensions, $D > 4$, there are new types of black objects. Beside the straightforward generalization of the Schwarzschild black hole to higher dimensions there are extended black objects as well. They extend infinitely in some directions (say along p spatial directions), while they are compact along the others. Black $p-$branes is the name of those objects. Black $p-$branes have the special and significant property that they are dynamically unstable objects, which is a fact known as the Gregory-Laflamme instability [34]. If one Fourier decomposes the linearized perturbations of black $p-$branes with respect to the time and the p extended spatial coordinates, one discovers an unstable mode

$$h_{ab} \sim \exp\left(\Omega t + i\vec{k} \cdot \vec{z}\right) , \tag{2.3.1}$$

(a mode which becomes larger and larger as time increases), for k smaller than a critical value $k \leq k_{GL}$. This implies that there are (probably) other solutions in the phase space of solutions to which the black $p-$brane may go to.

One can also generalize the Kerr black hole to higher dimensions, what is known as the Myers-Perry black hole [13]. There are two aspects of rotation that change significantly when spacetime has more than four dimensions. First, there is the possibility of rotation in several independent planes and, hence, there is the possibility of

7

several independent angular momenta. The other aspect of rotation that changes qualitatively as the number of dimensions increases is the relative competition between the gravitational and centrifugal potentials. The radial fall-off of the Newtonian potential "$-\frac{GM}{r^{D-3}}$" depends on the number of dimensions, whereas the centrifugal barrier "$\frac{J^2}{M^2 r^2}$" does not since rotation is confined to a plane. We see that the competition is different in $D = 4$, $D = 5$, and $D \geq 6$.

An interesting and important difference between higher dimensional black holes and four dimensional ones is the abscence of the Kerr-bound for some higher dimensional black holes. Some black holes can rotate very fast, with no upper bound. If you take, for example, a Myers-Perry black hole with a single rotation and make it rotate very fast then its horizon shape will pancake along the rotation plane, becoming a black $2-$brane in the limit [56]. Consequently, one learns that ultraspinning Myers-Perry black holes are unstable (in contrast to the the stable $4-$dim Kerr black holes), since black $p-$branes are unstable themselves.

The break-down of the uniqueness theorem in higher-dimensional general relativity was first displayed by the example of the five-dimensional black ring [14]. Now, with a given value of mass and angular momentum there is not only the rotating black hole with spherical topology, but also a black ring, thus breaking the uniqueness theorem. This example shows, furthermore, that black objects with topologies other than spherical can arise in higher dimensional general relativity. Later on, other composite black objects were found, with new topologies, like black saturn for example [15, 14]; a black hole at the center of a black ring. Di rings are another example of composite black objects in which one black ring is located inside a larger black ring, both with the same rotation plane [16].

As a result of the existence of different branches of solutions, each with a different topology, in some cases one may expect topological phase transitions between the different branches or phases. Examples of expected topological phase transitions are the pinch-down of a topologically spherical black hole to a black ring or to a black p-sphere, or the merger between black holes and black rings in black Saturns or di-rings in $D \geq 6$. How these phase transitions work or which mechanism is responsible for them, or whether there is something universal about those transitions in the phase space of higher dimensional black holes, are interesting questions deserving answers. In chapter 6 we give a detailed account of those, and also of similar phase transitions, and we give answers to the previous questions.

As was said in the previous section one may want, in addition, to make contact with the observed $4-$dimensional world. To this end, one needs to compactify the extra dimensions of spacetime, in a spirit similar to the Kaluza-Klein compactifications.

This gives rise to many interesting phenomena, part of which we are going to talk about in chapter 4. If one studies, for instance, the phase space of vacuum and static black hole solutions in 5−dimensional general relativity with the fifth dimension being compact (the internal compact manifold is a circle), one finds three special branches of solutions, the so called homogeneous black string phase, the inhomogeneous black string phase and the localized black holes phase. For certain values of the mass (for a fixed length of the circle) the three phases can exist, which is another example of how higher dimensional gravity breaks the uniqueness theorem. Here also, the phases are connected by a topological phase transition as explianed in chapter 4.

Finally, one can use the new features of higher dimensional general relativity to look for new approximate methods (special to higher dimensions) to construct new black hole solutions. A very successful approach is the blackfolds approach [27, 28, 66], which we are going to discuss in detial in chapter 3.

2.4   AdS/CFT correspondence

The AdS/CFT correspondence [17], or, more generally, the gauge-gravity duality is an equality between two theories; a quantum field theory in d spacetime dimensions and a gravity theory on a $d + 1$ dimensional spactime with a d dimensional boundary. The simplest example involves a conformal field theory (CFT) on the field theory side and the AdS spactime on the gravity side. Here, we are going to focus on the latter example, the AdS/CFT correspondence. The AdS_{d+1} metric in global coordinates can be written as

$$ds^2 = R^2 \left[- \left(r^2 + 1 \right) dt^2 + \frac{dr^2}{r^2 + 1} + r^2 d\Omega_{d-1}^2 \right] , \qquad (2.4.1)$$

where R is the radius of curvature of AdS_{d+1}. It is straightforward to see that the boundary of AdS_{d+1}, which is at $r >> 1$, is conformal to the cylinder $R \times S^{d-1}$. A conformal field theory, on the other hand, is a local quantum field theory invariant under the conformal group $SO(2, d)$, which includes the Poincare group, the dilatations, and special conformal transformations [18]. The AdS/CFT correspondence postulates that all the physics in an asymptotically AdS_{d+1} spacetime can be described by a conformal field theory that lives on the boundary $R \times S^{d-1}$. In other words, it relates a state of the field theory on the cylinder with a state of the bulk theory in global coordinates.

As for the conditions that are necessary for the duality we mention the following. A simple counting of degrees of freedom argument [19] shows that the number of fields on the field theory side is inversely proportional to the Newton's constant of the bulk. Since we want a weakly coupled theory in the bulk, so that gravity is a good

approximation, on the dual quantum field theory side this translates in demanding large N gauge theories, which are gauge theories based on the gauge group $SU(N)$ or, $U(N)$, with the fields in the adjoint representation.

However, the above is not a sufficient condition for the gravity to be a good approximation. In the gravity approximation we treat the graviton as a point-like particle and we ignore the string internal structure, thus we ignore the other massive string states. Namely, we assume that

$$R/\ell_s >> 1 \,, \tag{2.4.2}$$

where ℓ_s is the string length. If the above condition is not met then we should consider the full string theory. This condition translates in the field theory side into the requirement that the field theory should be strongly interacting, otherwise, light states of higher spin $S > 2$ will be generated, rendering the gravity approximation invalid. This is not sufficient though; the coupling should be large enough to give large energies to all higher spin particles.

As a concrete example we take the $3 + 1$ dimensional $\mathcal{N} = 4$ super Yang Mills / $\mathrm{AdS}_5 \times S^5$ duality. Here, the AdS_5 radius is given in terms of the Yang Mills quantities as follows

$$R^4/\ell_s^4 = 4\pi g_s N = g_{YM}^2 N = \lambda \,, \qquad R^4/\ell_p^4 = 4\pi N \,, \tag{2.4.3}$$

where g_{YM}^2 and λ are the Yang Mills coupling constant and the effective coupling constant (or the 't Hooft coupling), respectively, and ℓ_p is the planck length. As said previousely, for the gravity side to be weakly coupled one has to have $N >> 1$. Furthermore, one sees that to trust the gravity approximation the effective coupling constant has to be large. Thus, for $g_{YM}^2 N >> 1$ the gravity approximation is good and the field theory is strongly coupled, whereas for $g_{YM}^2 N << 1$ the gravity approximation is bad and the field theory is weakly coupled.

Finally, we mention, in brief, how the correspondence was derived in the first time. Look at the extremal black three-brane, or the black $D3-$brane, metric

$$ds^2 = f^{-1/2} \left(-dt^2 + \sum_{i=1}^{3} dx_i^2 \right) + f^{1/2} \sum_{i=1}^{6} dy_i^2 \,, \tag{2.4.4}$$

with

$$f = 1 + \frac{4\pi N \ell_p^4}{y^4} \,. \tag{2.4.5}$$

The coordinates x^i are the 3 spatial coordinates parallel to the 3-brane and the y^i are the six coordinates in the transvese direction. By y we mean $y \equiv \sqrt{\sum_{i=1}^{6} y_i^2}$. This description, in terms of extremal black branes, is valid when the string coupling is strong $g_s N >> 1$. For small string coupling $g_s N << 1$ the same system can be described

by a set of N $D-$branes [20] which is the non-perturbative regime of string theory since the α' corrections are large ($R/\ell_s << 1$). The conjecture is that the previous two descriptions are of one and the same system. This system can be described by either black branes or by D3 branes. At strong string coupling the D3-brane description is not valid and so it is better to describe the system by the gravity approximation which is valid then. At very small string coupling the gravity description breaks down, while the non-perturbative string theory is valid and so it is appropriate to descibe the system by D branes. Next, by taking the low energy limit of both descriptions one gets the gauge gravity correspondence upon identifying the two sides.

2.5   Fluid/Gravity correspondence

The Fluid/Gravity correspondence [21, 26] is a certain universal limit of the AdS/CFT correspondence in which the dynamics of the quantum field theory simplifies to that of an effective classical fluid dynamics. This can be done for any interacting quantum field theory at high enough temperatures by focusing on near-equilibrium dynamics and restricting attention to long wavelength physics. A qualitatively similar behaviour was discovered to take place in nature for the special state of matter produced in heavy-ions collisions at RHIC, known as the quark gluon plasam (QGP). This in turn requires the understanding of QCD at strong coupling, which is quite different from the class of superconformal field theories appearing in the AdS/CFT dualities, and hence the lessons one should draw (regarding the QGP) are only qualitatively true. The current understanding is that subsequent to the collision of ions, the resulting constituents of the system rapidly thermalize and come into local thermal equilibrium and so it evolves according to hydrodynamics until the local temperature falls back below the deconfinement temperature and the QGP hadronizes.

There is a rich literature on the investigation of linearized fluid dynamics from linearized gravity in asymptotically AdS black hole spacetimes, which started in the work [22]. In [30] the authors found that the ratio of shear viscosity to the entropy density of a large class of strongly interacting quantum field theories whose dual description involves black holes in AdS space is universal

$$\frac{\eta}{s} = \frac{1}{4\pi} \, , \tag{2.5.1}$$

and they even provided evidence that this ratio might stand as a lower bound for a large class of systems. The extension of this work to obtain non-linear fluid dynamics form gravity is what is known as the fluid-gravity correspondence. According to the gauge-gravity duality different asymptotically AdS bulk geometries correspond to different

states in the boundary theory. The pure AdS geometry, for instance, corresponds to the vacuum state of the gauge theory. A large Schwarzschild-AdS black hole corresponds to a state of global thermal equilibrium in the field theory. In more detail, in the field theory side, thermal equilibrium is characterized by a choice of static frame and temperature field. In the gravity side, on the other hand, the natural candidates for the equilibrium configuration are static (or stationary) black hole spacetimes. The temperature of the fluid would be given be by the Hawking temperature of the black hole and the velocity field of the fluid would be given by the boost velocity of the black hole; remember that if you take the radius of the Schwarzschild-AdS black hole to be very large it goes in the limit to a black brane, or to the planar black hole, for which a boost velocity is well-defined along the brane directions.

What one would like to do next is to deviate a little bit from thermal equilibrium, by letting the temperature and the velocity field of the black hole (and hence also the fluid) vary slowly along the boundary directions. A fluid slightly deviated from thermal equilibrium can be described in terms of transport coefficients, such as shear viscosity, bulk viscosity, relaxation times, etc. The consistent procedure in which this can be done (and the transport coefficents computed from the gravity side at the end) is the essence of the fluid-gravity correspondence which we are going to describe, in brief, below.

The fluid-gravity correspondence shows that the Einstein's equations, with a negative cosmological constant, supplemented with appropriate boundary conditions and regularity restrictions reduce to the non-linear equations of fluid dynamics in an appropriate regime of parameters. Start from the black $(d-1)-$brane solution in AdS_{d+1} space (the planar black hole). The solution is characterized by the temperature field T and the $d-1$ components of the velocity field u_i. By computing the Brwon-York stress tensor at the boundary one obtains a stress tensor of a perfect fluid, confirming the previous statement that a static black hole (here it is a homogeneous black brane) corresponds to global thermal equilibrium. By promoting the temperature field and the velocity field to slowly varying functions of the boundary coordinates x^μ, i.e., $T \to T(x^\mu)$ and $u_i \to u_i(x^\mu)$, and adding some corrections to the metric one gets a solution to the Einstein equations, with a negative cosmological constant, order by order in this derivative expansion method. The solution describes a dynamical and inhomogeneous black brane (a black brane slightly disturbed from complete spatial homogeneity and slowly evolving in time). This in turn corresponds in the field theory side to a dissipative fluid. Indeed, by computing now the Brown-York stress tensor at the boundary, in addition to the perfect fluid part, one obtains new dissipative pieces in the stress tensor of the fluid. At the one derivative level the fluid stress tensor

has a single undetermined parameter − the shear viscosity which one reads, using the gravity side, to be $\frac{\eta}{s} = \frac{1}{4\pi}$ as anticipated . At the two derivative level one determines other transport coefficients, such as the relaxation time for example. In this sense, the gravity side plays the role of choosing specific fluids as their dual by fixing the transport coefficients of the stress tensor to some values. Remember that by knowing the stress tensor of the fluid one can derive immediately its equations of motion as they are simply the conservation equations $\nabla_\mu T^{\mu\nu} = 0$.

2.6   Holography in flat space

Holography is supposed to be a universal feature of gravitational systems [7, 8]. Its formulation, however, in a general spacetime is understood only in very few cases. The most familiar and successful example of holography today is the asymptotically AdS spacetime. The AdS/CFT correspondence incorporates and exposes very nicely the holographic principle. There were many attempts, partially successful though, to define and formulate holography in deSitter spacetime. This is what has become known as the dS/CFT correspondence [23, 24]. There were very little progress, however, in formulating holography in asymptotically flat spacetimes, despite the fact that those spacetimes are the closest to intuition and to our experimental setups.

In hindsight, one of the immediately seen differences between the flat and AdS case is that in Anti-deSitter spacetime the boundary (where the dual theory lives) is timelike, whereas, in asymptotically flat spaces the smooth boundary of spacetime is null (future and past null infinity in the conformal Penrose diagram). This poses the difficulty of how, or even if it is possible at all, to formulate a dual quantum field theory on null surfaces. Some proposals for solving this problem and others were put forward by saying that the boundary of flat spacetime is spatial infinity instead (see [37, 38] and references therein). In [38], for example, it was argued that the dual quantum field theory to asymptotically flat spacetime is a non-local one.

In this regard, an interesting road to take would be to try to find the analoge of the fluid/gravity correspondence in flat space. Namely, take an asymptotically flat black brane (it is asymptotically flat only in the transverse directions of the brane) and try to find its dual fluid at spatial infinity, by making the brane fluctuate in a certain way, departing from homogeneity. An attempt in this direction can be found within the framework of the blackfolds approach [27, 28, 66], and, in particular, in what we are going to develop in chapter 5.

2.7 Outline of thesis

The outline of this thesis is the following:

- In chapter 3 we give a short introduction to the blackfolds approach to higher dimensional black holes. We dicuss the reasons that make new approximate methods available in higher dimensions. We intoduce the basic objects, or the building blocks, of the approach, which are the boosted black $p-$branes, and explain how the blackfolds approach can be used to construct from them new stationary solutions to the gravitational field equations with new and novel topologies and how it can be used to construct dynamical solutions as well.

- In chapter 4 we give a brief introduction to the topic of topology change in general relativity. We discuss the Kaluza-Klein black hole phases, the homogeneous black string phase, the inhomogeneous black string phase and the localized black hole phase. We explain the mechanism under which a topological phase transition appears as one moves in the phase space from a black string to a localized black hole.

- In chapter 5 we study long wavelength perturbations of neutral black p-branes in asymptotically flat space and show that, as anticipated in the blackfold approach, solutions of the relativistic hydrodynamic equations for an effective $p+1$-dimensional fluid yield solutions to the vacuum Einstein equations in a derivative expansion. Going beyond the perfect fluid approximation, we compute the effective shear and bulk viscosities of the black brane. The values we obtain saturate generic bounds. Sound waves in the effective fluid are unstable, and have been previously related to the Gregory-Laflamme instability of black p-branes. By including the damping effect of the viscosity in the unstable sound waves, we obtain a remarkably good and simple approximation to the dispersion relation of the Gregory-Laflamme modes, whose accuracy increases with the number of transverse dimensions. We propose an exact limiting form as the number of dimensions tends to infinity.

- In chapter 6 we study topology-changing transitions in the space of higher dimensional black hole solutions. Kol has proposed that these are conifold-type transitions controlled by self-similar double-cone geometries. We present an exact example of this phenomenon in the intersection between a black hole horizon and a cosmological deSitter horizon in $D \geq 6$. We also describe local models for the critical geometries that control many transitions in the phase space of

higher-dimensional black holes, such as the pinch-down of a topologically spherical black hole to a black ring or to a black p-sphere, or the merger between black holes and black rings in black Saturns or di-rings in $D \geq 6$.

- In chapter 7 we summarize our results.

- A and B are appendices belonging to chapter 6 .

Chapter 3

Blackfolds

3.1   General idea

The blackfolds approach to higher dimensional black holes [27, 28, 66] is an effective long-wavelength world-volume theory for the dynamics of black $p-$branes. It is analogous to the D.B.I action, which gives an effective description of the dynamics of $D-$branes when the deviations from the flat $D-$brane configuration are locally sufficiently small. Given a flat black $p-$brane in a background space, the blackfolds approach tells you how to bend this black $p-$brane over a submanifold W_p of the background manifold M_D, order by order in a certain derivative expansion, so as to make it a solution to the gravitational field equations. In this sense, the blackfolds approach can be used to construct new stationary solutions to the field equations with new topologies. A simple example of the latter idea is a black string in flat space. By boosting and curving the black string into a circle appropriately (to balance the forces), one obtains a black ring in flat space. A similar exercise can be performed in AdS and dS spaces [46]. One can use the blackfolds approach to study dynamical and non-stationary situations as well, as we are going to show in detail in chapter 5, and it turns to capture the Gregory-Laflamme instability of black $p-$branes in a very striking way.

The main reason why such constructions are not available in $4-$dimensional gravity is the fact that whereas in $4-$dimensions the length scales set by the mass and the angular momentum are of the same order of magnitude due to the Kerr bound $J \leq GM^2$, in higher dimensional gravity they can be largely separated since there are black holes with no upper bound on the angular momentum. The large separation in the length scales defines a small parameter which can be used to construct new solutions

order by order in the small parameter,

$$\frac{\ell_M}{\ell_J} << 1\,, \tag{3.1.1}$$

where ℓ_M and ℓ_J are the length scales associated with the mass and the angular momentum, respectively. For example, for neutral vacuum black holes one has

$$\ell_M \sim (GM)^{\frac{1}{D-3}}\,, \qquad \ell_J \sim \frac{J}{M}\,. \tag{3.1.2}$$

A familiar example of the previous dicussion is the Myers-Perry black hole. If one rotates it very fast and at the same time one keeps its horizon size finite then its horizon pancakes along the rotation plane and the resulting geometry is the infinitely extended, boosted flat black brane [56]. This example suggests that our building blocks should be the flat black $p-$branes as we are going to discuss in the next chapter.

One may want also to apply the blackfolds approach to construct new black hole solutions in supergravity and low energy string theory, stationary or dynamical. Here the test black objects (the blackfolds) can be charged with respect to different fields, of the types that arise in supergravity and string theory. This line was pursued in detail in [67, 68].

3.2   Boosted black $p-$branes

The building blocks of the blackfolds approach are the boosted black $p-$branes given by the metric

$$ds^2 = \left(\eta_{ab} + \frac{r_0^n}{r^n}u_a u_b\right)d\sigma^a d\sigma^b + \frac{dr^2}{1 - \frac{r_0^n}{r^n}} + r^2 d\Omega_{n+1}^2\,, \tag{3.2.1}$$

where one should remember, throughout, that the spacetime dimension D is given by

$$D = p + n + 3 \tag{3.2.2}$$

and where σ^a $(a = 0, ..., p)$ are the world-volume coordinates of the black $p-$brane. The collective coordinates of the black brane that describe its embedding in a background space are the horizon size r_0, the p spatial components of the velocity u^i satisfying $\eta_{ab}u^a u^b = -1$, and the embedding spacetime coordinate $X^\mu(\sigma)$ that specifies the location of the black brane inside the background space. The long-wavelength effective theory makes the variables (the collective coordinates) vary slowly along the submanifold W_p over a large length scale $R >> r_0$. Typically, R is set by the smallest curvature radius associated with W_p.

In general, upon such embeddings of branes in background spaces, promoting the variables to functions of the world-volume coordinates σ is also accompanied by changes in the world-volume metric (induced metric) $\eta_{ab} \to \gamma_{ab}(X^\mu(\sigma))$. Altogether one gets the following metric

$$ds^2 = \left(\gamma_{ab}(X^\mu(\sigma)) + \frac{r_0^n(\sigma)}{r^n} u_a(\sigma) u_b(\sigma) \right) d\sigma^a d\sigma^b + \frac{dr^2}{1 - \frac{r_0^n(\sigma)}{r^n}} + r^2 d\Omega_{n+1}^2 + ... \quad (3.2.3)$$

where the dots denote corrections of order $O(r_0/R)$ that make the metric solve the vacuum Einstein equations. In chapter 5 we are going to focus on the case where the black brane is in flat space and where only intrinsic fluctuations are allowed − no extrinsic bending of the brane is performed − so that $\gamma_{ab}(X^\mu(\sigma)) = \eta_{ab}$, and we are going to compute the first order corrections to the above metric. In ref [69] the authors studied the case in which one performs an extrinsic bending of the brane as well.

3.3 Effective stress tensor

The metric (3.2.3) is a solution to the field equations in what is called the near zone region, $r_0 \le r << R$, where the black brane degrees of freedom are dominant. On the other hand, in the far zone region, $r_0 << r \sim R$, the background space degrees of freedom dominates. Hence, the two metrics should match together in the matching zone, or the intermediate zone, where

$$r_0 << r << R. \quad (3.3.1)$$

Using the metric (3.2.3) one can compute a stress-energy tensor in the intermediate zone in accord to the Brown-York prescription [36],

$$T_{\mu\nu}^{(BY)} = \frac{1}{8\pi G} \left(K_{\mu\nu} - h_{\mu\nu} K - (K_{\mu\nu}^{(0)} - h_{\mu\nu} K^{(0)}) \right), \quad (3.3.2)$$

where $K_{\mu\nu}$ is the extrinsic curvature of the $r = $ constant surface, $h_{\mu\nu}$ is the induced metric on the surface , and where we perform a background substraction from flat spacetime. Furthermore, we can obtain an effective $p + 1$ stress tensor of the black brane by integrating out the short-wavelength degrees of freedom by integrating over the sphere S^{n+1}. That is, the effective $p + 1$ stress tensor is

$$T_{ab} = \int_{S^{n+1}} T_{ab}^{(BY)}. \quad (3.3.3)$$

At leading order in the expansion one obtains

$$T_{ab} = \frac{\Omega_{n+1}}{16\pi G} r_0^n (n u_a u_b - \eta_{ab}). \quad (3.3.4)$$

This is a stress tensor of a perfect fluid,

$$T_{ab} = (\rho + P) \, u_a u_b + P \eta_{ab} \,, \tag{3.3.5}$$

where the energy density and the pressure are

$$\rho = \frac{\Omega_{n+1}}{16\pi G}(n+1)r_0^n \,, \qquad P = -\frac{\Omega_{n+1}}{16\pi G}r_0^n \,. \tag{3.3.6}$$

One also defines local entopy and temperature,

$$s = \frac{\Omega_{n+1}}{4G}r_0^{n+1} \,, \qquad T = \frac{n}{4\pi r_0} \,. \tag{3.3.7}$$

The thermodynamics of black holes is satisfied locally on the black brane. The first law of thermodynamics is satisfied locally,

$$d\rho = Tds \,, \tag{3.3.8}$$

and also the the Euler-Gibbs-Duhem relation,

$$\rho + P = Ts \,. \tag{3.3.9}$$

3.4 Equations of motion for blackfolds

Finally, we list below a couple of results in a short manner. The blackfolds equations of motion split into extrinsic and intrinsic equations respectively,

$$T^{\mu\nu}K_{\mu\nu}{}^{\rho} = 0 \,, \tag{3.4.1}$$

$$D_a T^{ab} = 0 \,, \tag{3.4.2}$$

where $a, b, ...$ are world-volume indices and $\mu, \nu, ...$ are spacetime indices. In the above we have used the following definitions. $T^{\mu\nu}$ is the pullback tensor constructed from T^{ab} as

$$T^{\mu\nu} = \partial_a X^\mu \partial_b X^\nu T^{ab} \,. \tag{3.4.3}$$

The tensor $K_{\mu\nu}{}^{\rho}$ is the extrinsic curvature tensor defined as

$$K_{\mu\nu}{}^{\rho} = h_\mu{}^\sigma h_\nu{}^\alpha \nabla_\alpha h_\sigma{}^\rho \,, \tag{3.4.4}$$

where $h^{\mu\nu}$ is the first fundamental form of the submanifold W_{p+1} given by

$$h^{\mu\nu} = \partial_a X^\mu \partial_b X^\nu \gamma^{ab} \,. \tag{3.4.5}$$

Finally, D_a is the world-volume covariant derivative.

Chapter 4

Topology change in general relativity

4.1 Prelude

As is well known, in 4−dimensional gravity there is the uniqueness theorem [9], which states, in special, that for vacuum Einstein equations, for a given mass and angular momentum there is only one black hole solution, the Schwarzschild-Kerr black hole, which has a horizon topology of a 2−shpere. In higher dimensions however, for spacetime dimension D larger than four, the uniqueness theorem does not hold, and a counter example was found; the 5−dimensional black ring [14]. In 5−dimensions, for a given mass and angular momentum, in addition to the Myers-Perry black hole solution there are two black ring solutions as well. Another example of the break down of the uniqueness theorem in higher dimensions is the phase space of static and neutral Kaluza-Klein black holes, which is going to be the focus of our current chapter. The known phases insofar are the socalled (1) the uniform black string (2) the nonuniform black string (3) the localized black hole, and a class of phases which is called (4) the Kaluza-Klein bubbles. For certain values of the mass three solutions exist, a uniform black string, a nonuniform black string and a localized black hole, the latter having a topology different from the former two phases. As for the phases of Kaluza-Klein bubbles we refer the reader to [71] and we content ourselves by saying that there, there is even a continuousely infininte non-uniqueness of solutions .

As was just mentioned, in this chapter, for simplicity, we are going to focus on static and neutral Kaluza-Klein black holes. For reviews including charged and rotating Kaluza-Klein black holes see for example [70].

4.2 Phases of Kaluza-Klein black holes

A $(d+1)-$dimensional static and neutral Kaluza-Klein black hole is defined as a vacuum gravity solution that asymptotes to d dimensional Minkowski spacetime times a circle S^1. That is, at infinity it is $M_d \times S^1$. There are 3 branches of solutions that share the property that they have a local $SO(d-1)$ symmetry and they are the:

(i) Uniform black string

(ii) Nonuniform black string

(iii) Localized black hole

and there is a quite distinct further class of phases (for which we refer the reader to [71]), called the Kaluza-Klein bubbles. In what follows we give an account of each of the three phases in some detail.

(i) The uniform black string solution is a familiar one, and its metric is

$$ds^2 = -\left(1 - \frac{r_0^{d-3}}{r^{d-3}}\right)dt^2 + \frac{dr^2}{1 - \frac{r_0^{d-3}}{r^{d-3}}} + r^2 d\Omega_{d-2}^2 + dz^2\,, \qquad (4.2.1)$$

with the coordinate z having the compact range

$$z \in [0, L]\,, \qquad (4.2.2)$$

where L is the length of the Kaluza-Klein circle S^1. The topology of the horizon of the uniform black string is

$$S^{d-2} \times S^1\,. \qquad (4.2.3)$$

For fixed L, the black string solution exist for every size of the horizon r_0. Nevertheless, for sufficiently small black strings (r_0 sufficiently small relative to L) the uniform black string is unstable due to the Gregory-Laflamme instability, whereas for sufficiently large r_0 the uniform black string is stable. In other words, for fixed L and d, there is a certain size of the horizon $r_0 = L_{GL}$ such that for $r_0 < L_{GL}$ the uniform black string is unstable while for $r_0 > L_{GL}$ it becomes stable.

In the range $r_0 < L_{GL}$, which is equivalent to say, for small masses, if one perturbes the uniform black string, then the Gregory-Laflamme instability takes the uniform black string to another solution. However, as the Gregory-Laflamme mode is time dependent in this range, one will be moving in the phase space of solutions along a trajectory of time dependent solutions. The latter trajectory, however, lies outside the static configuration space we are interested in. In short, in this range the uniform black string is dynamically unstable.

In the range $r_0 > L_{GL}$, that is, for large masses, the uniform black string is stable, but agian, since perturbations are time dependent the resulting perturbed solutions are dynamical (they will decay to the uniform black string after some time) and so these configurations fall short of our interest.

The marginal value $r_0 = L_{GL}$ is interesting and it gives rise to the nonuniform black string phase, which we will discuss next.

(ii) At the the marginal value $r_0 = L_{GL}$ something interesting happens to the uniform black string. As the perturbation mode is time independent for this marginal value one expects to move from the uniform black string configuration to another static configuration in which the black string size varies along the Kaluza-Klein circle. This phase is called the inhomogeneous black string phase or the nonuniform black string phase. Since this phase is connected continuously to the uniform phase, the topology of the nonuniform black string is the same as the uniform one, $S^{d-2} \times S^1$, at least when the deformation away from the uniform black string is sufficiently small. This solution was found numerically in [49].

(iii) Note that one can localize on the Kaluza-Klein circle a black hole of topology S^{d-1} if its size is very small compared to the length of the circle L. For regions close enough to the black hole, the black hole can be approximated by the familiar Schwarzschild solution in $d+1$ dimensions

$$ds^2 = -\left(1 - \frac{R_0^{d-2}}{r^{d-2}}\right) dt^2 + \frac{dr^2}{1 - \frac{R_0^{d-2}}{r^{d-2}}} + r^2 d\Omega_{d-1}^2 \,, \qquad (4.2.4)$$

where R_0 is the Schwarzschild radius of the black hole. For $R_0 << L$ an analytical solution was found in [72, 73] up to first order. There has been also some numerical work on this branch (see for example [74, 75]).

Note that this phase corresponds to small masses in the parameter space. Since the uniform black string is dynamically unstable in this range, one expects the localized black hole to be the end state of that instability. Therefore, one expects the localized black hole to be dynamically stable.

4.3   Black string−black hole transition

Upon taking the localized black hole and starting to increase its size (its mass) little by little, at some point the two ends of the black hole will touch each other across the Kaluza-Klein circle. After its two ends intersect one expects them to merge. Note that the configuration with the two ends of the black hole merged is no more than a

nonuniform black string configuration. Therefore, one clearly sees that, the nonuniform black string phase connects the localized black hole phase with the uniform black string phase, each with a different topology, and hence one expects to encounter, here, a topological phase transition.

One can also imagine the opposite direction scenario. Start from a nonuniform black string solution, and increase its inhomogeneity little by little, in such a way as to make the horizon shrink to zero size, or pinch off, at some place along the Kaluza-Klein circle. The resulting solution is a large localized black hole with its two ends just touching across the circle. The next point along this phase space trajectory is a localized black hole with its two ends seperated from each other. Here again, the nonuniform phase behaves as a mediator upon moving, in the phase space, from the uniform phase to the localized phase.

It was argued in [52] that the solution that mediates between the two different topology solutions is singular. Locally, at the point where the two ends of a large localized black hole intersect an exact solution was proposed. It is a Ricci-flat self-similar cone, which can be written in the Euclidean section as

$$ds^2 = dz^2 + \frac{z^2}{D-2} \left[d\Omega_2^2 + (D-4)d\Omega_{D-3}^2 \right] , \qquad (4.3.1)$$

which is a cone over $S^2 \times S^{D-3}$. The Lorentzian version is,

$$ds^2 = dz^2 + \frac{z^2}{D-2} \left[-\sin^2 \beta dt^2 + d\beta^2 + (D-4)d\Omega_{D-3}^2 \right] . \qquad (4.3.2)$$

with $\beta \in [0, 2\pi]$. The cone is singular at the apex, at $z = 0$. There are two horizons, one at $\beta = 0$ and the other at $\beta = \pi$, and they are connected, not smoothly, at the apex of the cone $z = 0$. Note, furthermore, that both the S^2 and the S^{D-3} are contractible since their sizes shrink to zero at the apex. There are two ways to deform the cone so as to turn it into a smooth geometry (see figure 4.1 below). The first way is to go to the nonuniform black string phase, by resolving the S^{D-3}, i.e., by making it not contractible, leaving the Euclidean S^2 contractible. The second way is to go to the localized black hole phase, by resolving the Euclidean S^2, i.e., by making it not contractible, leaving the S^{D-3} contractible. See the figure 4.1, below, for illustration.

The cone metric written above is the local critical geometry around the intersection point. As for the critical geometry away from the intersection point, no analytical results were obtained, and people have resorted, instead, to numerical work (e.g. see [74] and references therein).
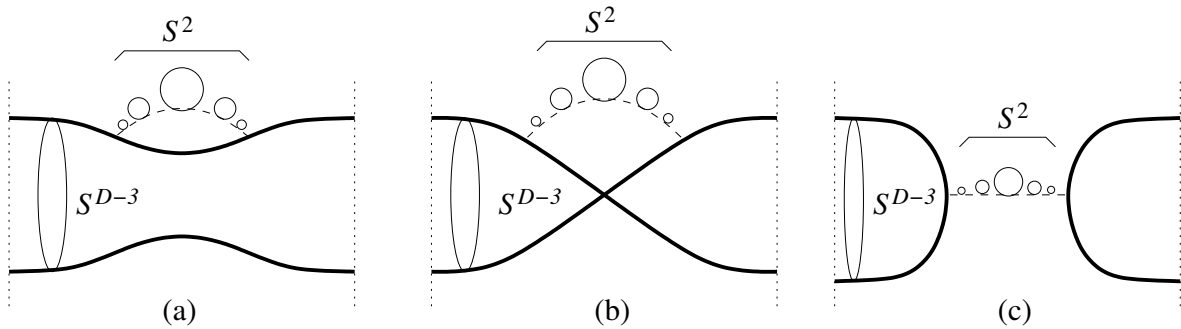
Figure 4.1: Black hole/black string transition in a Kaluza-Klein circle (the circle runs along the horizontal axis), following [52]. The circle fibered over the dashed segments is the Euclidean time circle, which shrinks to zero at the horizon: this fiber bundle describes a S^2. We also mark a cycle S^{D-3} on the horizon. In the black string phase (a) the S^2 is contractible, the S^{D-3} is not, while in the black hole phase (c) the S^{D-3} is contractible, the S^2 is not. The transition between the two phases is of conifold type, with the critical geometry (b) becoming, near the pinch-off point, a cone over $S^2 \times S^{D-3}$.

4.4   Other topological transitions

In chapter 6 we are going to provide an exact analytical example of a topological phase transition of a different, but analogous, system in which the transition is mediated, as well, by a self-similar cone; a rotating black hole in deSitter space with a single rotation in $D \geq 6$. In other words, we are going to give the full geometries (not only the local ones) along the transition trajectory in the phase space of solutions, starting from a regular phase of two disconnected horizons, to a critical geometry (singular) of two intersecting horizons, and finally to a merged phase with a single horizon.

We are also going to describe in chapter 6 local models for the critical geometries that control many transitions in the phase space of higher-dimensional black holes, such as the pinch-down of a topologically spherical black hole to a black ring or to a black p-sphere, or the merger between black holes and black rings in black Saturns or di-rings in $D \geq 6$.

Chapter 5

Black Brane Viscosity and the Gregory-Laflamme Instability

5.1 Introduction and Summary

Black holes exhibit thermodynamic behavior, so it is natural to expect that their long wavelength fluctuations, relative to a suitable length scale, can be described using an effective hydrodynamic theory. Over the years there have appeared several different realizations of this idea, which differ in the precise set of gravitational degrees of freedom that are captured hydrodynamically (*e.g.,* only those inside a (stretched) horizon as in [25], or the entire gravitational field up to a large distance from a black brane spacetime as in [26, 27]) or in the kind of asymptotics (Anti-deSitter [26] or flat [27]) of the black hole/brane geometry.

In this chapter we focus on the hydrodynamic formulation developed recently for higher-dimensional black holes, including asymptotically flat vacuum black holes and black branes [27]. In this approach the effective stress tensor of the 'black brane fluid' is the quasilocal stress tensor computed on a surface B in a region that is asymptotically flat in directions transverse to the brane[1]. The equations of stress-energy conservation describe both hydrodynamic (intrinsic) fluctuations along the worldvolume of the brane, and elastic (extrinsic) fluctuations of the brane worldvolume inside a 'target' spacetime that extends beyond B. Thus the dynamics of a black p-brane takes the form of the dynamics of a fluid that lives on a dynamical worldvolume. This is referred to as the blackfold approach.

In this chapter we only study the intrinsic, hydrodynamic aspects of the brane. The worldvolume geometry, defined by the surface B at spatial infinity, is kept flat

---

[1]In the following, asymptotic flatness always refers to directions transverse to the brane.

and fixed. Fluctuations of the worldvolume geometry are non-normalizable modes, so the extrinsic worldvolume dynamics decouples. With this simplification, the set up is very similar to the fluid/AdS-gravity correspondence of [26], which we follow in many respects. The main difference is that we consider vacuum black brane solutions, with no cosmological constant and with different asymptotics.

The quasilocal stress tensor of a neutral vacuum black brane, with geometry equal to the $n + 3$-dimensional Schwarzschild-Tangherlini solution times $\mathbb{R}^p$, is that of a perfect fluid with energy density ρ and pressure P related by the equation of state

$$P = -\frac{\rho}{n+1}\,. \tag{5.1.1}$$

We may choose the black brane temperature T as the variable that determines ρ and P. The brane could also be boosted and thus have a non-zero velocity field along its worldvolume. In a stationary equilibrium state, the temperature and the velocity are uniform. We study fluctuations away from this state where these quantities vary slowly over the worldvolume. Their wavelength is measured relative to the thermal length T^{-1}, so for a fluctuation with wavenumber k the small expansion parameter is

$$\frac{k}{T} \ll 1\,. \tag{5.1.2}$$

Since for a vacuum black brane the temperature is inversely proportional to the thickness of the brane, r_0, this can be equivalently expressed as $kr_0 \ll 1$.

To leading order in this expansion we obtain the hydrodynamics of an effective perfect fluid, which refs. [28, 27, 29] have used to derive non-trivial results for higher-dimensional black holes. At the next order the stress tensor includes dissipative terms. For the purely intrinsic dynamics, these are the shear and bulk viscosities, η and ζ. In contrast to [26], our fluid is not conformally invariant so $\zeta \neq 0$ is expected.

By analyzing long wavelength perturbations of the black brane and their effect on the stress tensor measured near spatial infinity we obtain

$$\eta = \frac{s}{4\pi}\,, \qquad \zeta = 2\eta\left(\frac{1}{p} - c_s^2\right) \tag{5.1.3}$$

where s is the entropy density of the fluid, *i.e.*, $1/4G$ times the area density of the black brane, and

$$c_s^2 = \frac{dP}{d\rho} = -\frac{1}{n+1} \tag{5.1.4}$$

is the speed of sound, squared.

Written in the form (5.1.3), these values for η and ζ saturate the bounds proposed in [30] and [31]. The result for the shear viscosity is not too surprising: η can be argued to depend only on the geometry near the horizon and its ratio to s is universal for theories

of two-derivative Einstein gravity [30, 32] (see also [33]). The bulk viscosity, instead, does depend strongly on the radial profile transverse to the brane[2] so the saturation of the bound is presumably less expected. Note, however, that these black branes have different asymptotics than in all the previous instances where the effective viscosities of black branes have been considered. In particular, these black branes presumably are not dual to the plasma of any (local) quantum field theory. In any case it is worth emphasizing that our computations are for the theory with the simplest gravitational dynamics: $R_{\mu\nu} = 0$.

The imaginary speed of sound (5.1.4) implies that sound waves along the effective black brane fluid are unstable: under a density perturbation the fluid evolves to become more and more inhomogenous. Since this means that the black brane horizon itself becomes inhomogeneous, ref. [27] related this effect to the Gregory-Laflamme (GL) instability of black branes [34][3]. Then (5.1.4) implies a simple form for the dispersion relation of the GL unstable modes $\omega(k) = -i\Omega(k)$ at long wavelength: $\Omega = k/\sqrt{n+1} + O(k^2)$, i.e., the slope of the curve $\Omega(k)$ near $k = 0$ is exactly (and very simply) determined in the unstable-perfect-fluid approximation.
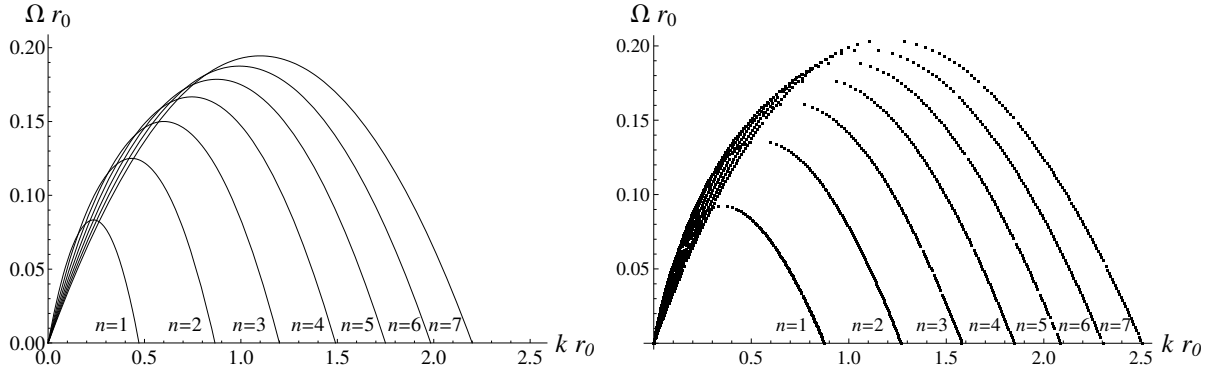
Figure 5.1: Left: dispersion relation $\Omega(k)$, eq. (5.1.5), for unstable sound waves in the effective black brane fluid (normalized relative to the thickness r_0). Right: $\Omega(k)$ for the unstable Gregory-Laflamme mode for black branes (numerical data courtesy of P. Figueras). For black p-branes in D spacetime dimensions, the curves depend only on $n = D - p - 3$.

Using our results for η and ζ we can include the viscous damping of sound waves in the effective black brane fluid. The dispersion relation of unstable modes becomes

$$\Omega = \frac{k}{\sqrt{n+1}} \left(1 - \frac{n+2}{n\sqrt{n+1}} kr_0 \right), \tag{5.1.5}$$

---

[2]For instance, in the membrane paradigm the bulk viscosity on the stretched horizon for a generic black hole turns out to be negative. Our result (5.1.3) is instead positive.

[3]This connection had also been made for black branes with gauge theory duals in [35].

29

which is valid up to corrections $\propto k^3$. Figure 5.1 compares this dispersion relation to the numerical results obtained from linearized perturbations of a black p-brane. Zooming in on small values of kr_0, the match is excellent. When kr_0 is of order one
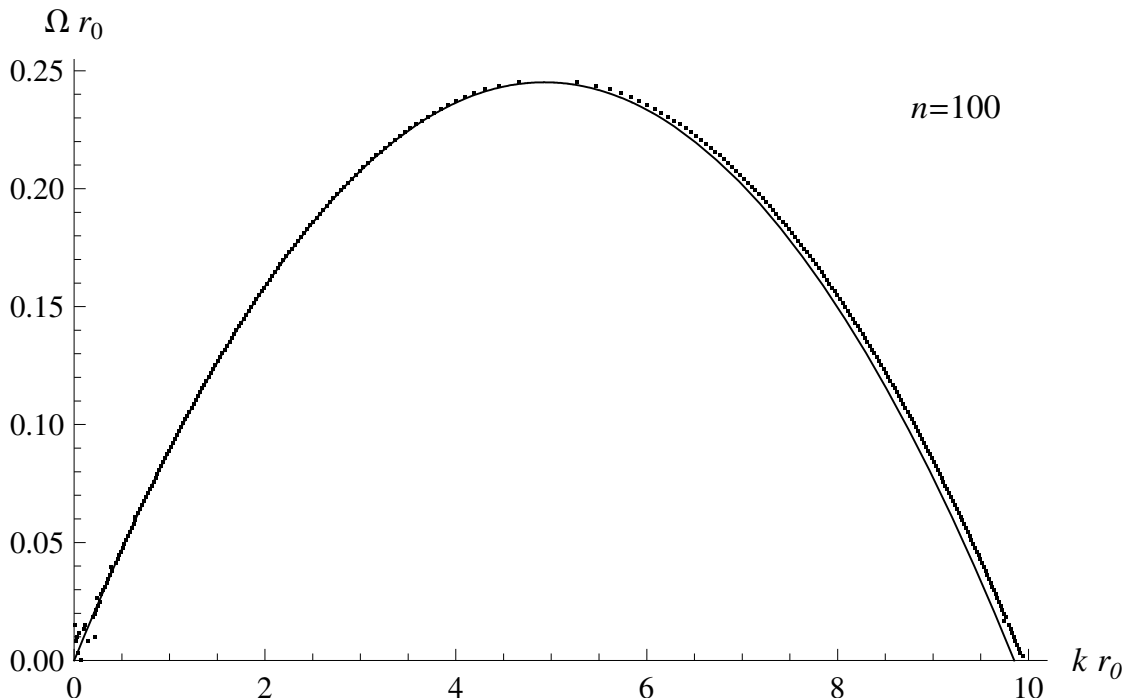
Figure 5.2: Dispersion relation $\Omega(k)$ of unstable modes for $n = 100$: the solid line is our analytic approximation eq. (5.1.5); the dots are the numerical solution of the Gregory-Laflamme perturbations of black branes (numerical data courtesy of P. Figueras).

we have no right to expect agreement, but the overall qualitative resemblance of the curves is nevertheless striking. The quantitative agreement improves with increasing n and indeed, as figure 5.2 shows, at large n it becomes impressively good over all wavelengths: for $n = 100$ the numerical values are reproduced to better than 1% accuracy up to the maximum value of k. Although the extent of this agreement is surprising, we will provide some arguments for why the fluid approximation appears to be so successful as n grows.

Thus, the effective viscous fluid seems to capture in a simple manner some of the most characteristic features of black brane dynamics. We believe this is a significant simplification from the complexity of the full Einstein equations.

The outline of the rest of the chapter is as follows: the next section contains the bulk of the calculations of the paper for a generic hydrodynamic-type perturbation of the black brane. We highlight the differences with the analysis of [26], in particular at

asymptotic infinity, and compute the values (5.1.3) for the effective η and ζ. Section 5.3 relates the linearized damped sound-mode perturbations of the fluid to the Gregory-Laflamme perturbations of the black brane. We examine the conditions that can lead to the surprising quantitative agreement of the dispersion relation at large n, and we propose its exact form as $n \to \infty$. We close in section 5.4 with an examination of the differences with other fluid-like approaches to the GL instability, and a discussion of our results within the context of the blackfold approach.

5.2   Hydrodynamic perturbations of black branes

In this section we study general perturbations of a vacuum black p-brane with slow variation along the worlvolume directions of the brane. Up to gauge transformations, they are fully determined by the boundary conditions of horizon regularity and asymptotic flatness at spatial infinity. Most of our analysis is very close to the study of hydrodynamic perturbations of AdS black branes, but there is an additional complication in the study of the perturbations at asymptotic infinity. Nevertheless, we are able to find the complete explicit form of the perturbed solution for a generic hydrodynamic flow to first order in the derivative expansion.

Readers who do not need or want the technical details of the calculation of the perturbed solution and the viscous stress tensor can safely skip to section 5.3.

5.2.1   Preliminaries

Black branes and their effective stress tensor

The black p-brane solution of vacuum gravity in $D = p + n + 3$ dimensions is

$$ds^2 = \left(\eta_{ab} + \frac{r_0^n}{r^n} u_a u_b \right) d\sigma^a d\sigma^b + \frac{dr^2}{1 - \frac{r_0^n}{r^n}} + r^2 d\Omega_{n+1}^2 \,, \tag{5.2.1}$$

with $a = 0, 1, \ldots, p$. The solution is characterized by the horizon radius r_0 (or brane 'thickness') and the worldvolume velocity u^a, with $u^a u^b \eta_{ab} = -1$. It is asymptotically flat in the directions transverse to the worldvolume coordinates σ^a. We can associate to it a stress-energy tensor measured at spatial infinity. There are several possible definitions of this stress tensor that would be equivalent for calculational purposes, but for conceptual reasons the most convenient for us is the quasilocal one of Brown and York [36]. We consider a boundary surface at large constant r, with induced metric $h_{\mu\nu}$ and compute

$$T_{\mu\nu}^{(\mathrm{BY})} = \frac{1}{8\pi G} \left(K_{\mu\nu} - h_{\mu\nu} K - (K_{\mu\nu}^{(0)} - h_{\mu\nu} K^{(0)}) \right) \,, \tag{5.2.2}$$

31

where $K_{\mu\nu}$ is the extrinsic curvature of the surface and we perform a background substraction from flat spacetime.

The geometry of the boundary surface for (5.2.1) is $\mathbb{R}^{1,p} \times S^{n+1}$. We will introduce perturbations with wavelengths much longer than the size r_0 of the S^{n+1} at the horizon. The deformations of this sphere all have large masses $\sim 1/r_0$ and therefore decouple. Thus the $SO(n+2)$ symmetry of S^{n+1} is preserved and, in an appropriate gauge, the metric will remain a direct product with a factor of this sphere. We integrate over the sphere to obtain the stress tensor for the black p-brane

$$T_{ab} = \int_{S^{n+1}} T_{ab}^{(\mathrm{BY})} \,. \tag{5.2.3}$$

We regard this stress tensor as living on the worldvolume of the brane, $i.e.,$ the $p+1$ extended directions of the boundary. The worldvolume metric results from the asymptotic form of the boundary metric, which in our case is the Minkowski metric

$$h_{ab} \to \eta_{ab} \,. \tag{5.2.4}$$

A main advantage of using the quasilocal stress tensor is that the Gauss-Codacci equations for the constant-r cylinder imply $\partial^a T_{ab} \propto R^r{}_b$, so imposing the Einstein equations in vacuum it follows that the stress tensor is conserved

$$\partial^a T_{ab} = 0 \,. \tag{5.2.5}$$

The stress tensor for the solution (5.2.1) has the perfect fluid form

$$T_{ab} = \rho u_a u_b + P P_{ab} \,, \qquad P_{ab} = \eta_{ab} + u_a u_b \tag{5.2.6}$$

with energy density and pressure

$$\rho = -(n+1)P = (n+1)\frac{\Omega_{n+1} r_0^n}{16\pi G} \,. \tag{5.2.7}$$

The horizon area allows to associate a local entropy density to this effective fluid

$$s = \frac{\Omega_{n+1} r_0^{n+1}}{4G} \tag{5.2.8}$$

and all the thermodynamic functions can be expressed as functions of the temperature

$$T = \frac{n}{4\pi r_0} \,. \tag{5.2.9}$$

We can equivalently use T or r_0 as the variable that determines local equilibrium. In this section we will mostly use r_0 for notational simplicity.

32

We will be interested in preserving regularity at the horizon. This is manifest if instead of the Schwarzschild coordinates in (5.2.1) we use Eddington-Finkelstein (EF) ones,

$$\sigma^a \to \sigma^a - u^a r_* , \qquad r_* = \int \frac{1}{1 - (r_0/r)^n} dr , \tag{5.2.10}$$

such that

$$ds^2 = -\left(1 - \frac{r_0^n}{r^n}\right) u_a u_b d\sigma^a d\sigma^b - 2u_a d\sigma^a dr + P_{ab} d\sigma^a d\sigma^b + r^2 d\Omega_{n+1}^2 . \tag{5.2.11}$$

Perturbations

We promote the thickness and velocity parameters to collective fields over the world-volume, so

$$ds_{(0)}^2 = -\left(1 - \frac{r_0(\sigma)^n}{r^n}\right) u_a(\sigma) u_b(\sigma) d\sigma^a d\sigma^b - 2u_a(\sigma) d\sigma^a dr + (\eta_{ab} + u_a(\sigma) u_b(\sigma)) d\sigma^a d\sigma^b$$
$$+ r^2 d\Omega_{n+1}^2 , \tag{5.2.12}$$

where $r_0(\sigma)$ and $u^a(\sigma)$ are assumed to vary slowly relative to the scale set by r_0. In this chapter we expand them to first order in derivatives, which we keep track of through a formal derivative-counting parameter ϵ. With non-uniform r_0 and u^a, the metric (5.2.12) is not Ricci flat so we add to it a component with radial dependence

$$ds^2 = ds_{(0)}^2 + \epsilon f_{\mu\nu}(r) dx^\mu dx^\nu + O(\epsilon^2) . \tag{5.2.13}$$

We choose a gauge in which ∂_r is a null vector with normalization fixed by the radius r of S^{n+1}, so that

$$f_{rr} = 0 , \qquad f_{\Omega\mu} = 0 . \tag{5.2.14}$$

With this choice the sphere S^{n+1} can be integrated out.

Demanding that (5.2.13) satisfies the vacuum Einstein equations to first order in ϵ results into a set of ODEs for $f_{\mu\nu}(r)$. These will be solved subject to regularity at the horizon $r = r_0$, which is easily imposed as a condition of metric finiteness in EF coordinates, and to asymptotic flatness, to which we turn next.

Asymptotic infinity

The asymptotic behavior of our spacetimes introduces an important difference relative to the perturbations of AdS black branes. For the latter, the calculations can be performed in their entirety in EF coordinates in which ∂_r is a null vector. By taking large values of r in these coordinates one approaches null infinity, but in AdS this is

the same as spatial infinity. The AdS boundary is always a timelike surface. However, in our asymptotically flat space, null and spatial infinities differ.

We are ultimately interested in computing the quasilocal stress tensor on a timelike boundary of spacetime endowed with a non-degenerate metric. But if we approach null infinity, the boundary metric will be degenerate and it is unclear whether the quasilocal stress tensor is well defined there. Instead, it seems more appropriate (and is definitely unproblematic) to compute the stress tensor at spatial infinity[4]. For this purpose EF coordinates are very awkward and it is much more convenient to switch back to Schwarzschild-like coordinates $\{r, t, \sigma^i\}$ at large r.

Thus we will work with two sets of coordinates: EF ones, in which horizon regularity is manifest, and Schwarzschild coordinates, in which spatial infinity is naturally approached. We need to provide the change of coordinates that relates them, extending the inverse of (5.2.10) to include $O(\epsilon)$ terms. The correction is naturally guessed by recalling that u^a and r_0, which appear in the transformation (5.2.10), now depend on the EF coordinates. Thus,

$$\sigma^a \to \sigma^a + u^a(v, \sigma^i) \int \frac{dr}{1 - (r_0(v, \sigma^i)/r)^n} \,, \tag{5.2.15}$$

or more explicitly,

$$v \to t + r_* + \epsilon \frac{(t + r_*)\partial_v r_0 + \sigma^i \partial_i r_0}{r_0} \left(r_* - \frac{r}{1 - (r_0/r)^n} \right) + O(\epsilon^2) \,,$$
$$\sigma^i \to \sigma^i + \epsilon \left((t + r_*)\partial_v u^i + \sigma^j \partial_j u^i \right) r_* + O(\epsilon^2) \,. \tag{5.2.16}$$

5.2.2 Solving the perturbation equations

At each point we choose coordinates centered on that point and go to an (unperturbed) local rest frame. In EF coordinates the velocity perturbation is

$$u^v(\sigma) = 1 + O(\epsilon^2) \,, \qquad u^i(\sigma) = \epsilon \sigma^a \partial_a u^i(0) + O(\epsilon^2) \,. \tag{5.2.17}$$

Note that since local velocities are small the constraint $u^2 = -1$ is automatically satisfied to the order we need. The other collective variable of the effective black brane

---

[4]Presumably the appropriate notion of spatial infinity here is not Penrose's i^0 (which is just a point) but more along the lines of [37], which naturally allows a dependence along the boundary directions. Although our spatial infinity is not exactly the same as in [37] since instead of a hyperboloid we work on a cylinder where $\mathbb{R}^{1,p}$ and S^{n+1} scale differently at infinity, this is not a problem for us since we are integrating over S^{n+1}. It would be interesting, especially with a view to holography, to further formalize this notion of spatial infinity. Related remarks concerning holography in asymptotically flat spacetimes have been made in [38].

fluid is the temperature T, or equivalently the thickness r_0, which we perturb as

$$r_0(\sigma) = r_0(0) + \epsilon\sigma^a\partial_a r_0(0) + O(\epsilon^2)\,. \tag{5.2.18}$$

In the following we understand all quantities as evaluated at $\sigma^a = 0$ and thus denote $\partial_a u^i(0) \to \partial_a u^i$, $r_0(0) \to r_0$ etc.

The metric (5.2.13) is now

$$\begin{aligned}
ds^2 =&\, 2dvdr - f(r)dv^2 + \sum_{i=1}^{p} d\sigma_i^2 + r^2 d\Omega_{n+1}^2 \\
&- 2\epsilon\sigma^a\partial_a u_i d\sigma^i dr + \epsilon\frac{nr_0^{n-1}\sigma^a\partial_a r_0}{r^n}dv^2 - 2\epsilon\frac{r_0^n\sigma^a\partial_a u_i}{r^n}d\sigma^i dv + \epsilon f_{\mu\nu}(r)dx^\mu dx^\nu\,,
\end{aligned} \tag{5.2.19}$$

where we denote

$$f(r) = 1 - \frac{r_0^n}{r^n}\,. \tag{5.2.20}$$

The Einstein equations with a radial index, $R^r{}_a = 0$ do not involve second derivatives and are constraint equations. Indeed they only involve the hydrodynamic fields r_0 and u^i and not $f_{\mu\nu}$,

$$(n+1)\partial_v r_0 = -r_0\partial^i u_i\,, \qquad \partial_i r_0 = r_0\partial_v u_i\,, \tag{5.2.21}$$

so they are to be regarded as the equations of fluid dynamics, consistently with (5.2.5). We also verify this interpretation later.

The remaining Einstein's equations are dynamical and we solve them to find $f_{\mu\nu}$. The equations $R_{ij} = 0$ give

$$\partial_r\left(r^{n+1}ff_{ij}{}'\right) = -2(n+1)r^n\partial_{(i}u_{j)}\,, \tag{5.2.22}$$

which, requiring finiteness at the horizon, are solved by

$$f_{ij}(r) = c_{ij} - 2\partial_{(i}u_{j)}\left(r_* - \frac{r_0}{n}\log f\right)\,. \tag{5.2.23}$$

The integration constants c_{ij} will be fixed later demanding asymptotic flatness. The equations $R_{vi} = 0$,

$$\partial_r\left(r^{n+1}f_{vi}{}'\right) = -(n+1)r^n\partial_v u_i\,, \tag{5.2.24}$$

are solved by

$$f_{vi} = c_{vi}^{(2)} + \frac{c_{vi}^{(1)}}{r^n} - \partial_v u_i r\,, \tag{5.2.25}$$

which are regular at the horizon for all values of the constants. Next, the equations from $R_{rr} = 0$ and $R_{\Omega\Omega} = 0$ are

$$f_{vr}{}' = \frac{r}{2(n+1)}\sum_{i=1}^{p} f_{ii}{}''\,, \tag{5.2.26}$$

35

and

$$\partial_r \left(r^n f_{vv} \right) = r^n \partial^i u_i + \frac{r^n f}{2} \left(\sum_{i=1}^{p} f_{ii}{}' - 2f_{vr}{}' \right) - 2nr^{n-1} f_{vr} , \tag{5.2.27}$$

which, assuming that eqs. (5.2.21) are satisfied, are solved by

$$f_{vr} = c_{vr} + \frac{r^2}{2(n+1)} \frac{d}{dr} \sum_i \frac{f_{ii}}{r} , \tag{5.2.28}$$

and

$$f_{vv} = \frac{2\partial^i u_i r + \left(1 - \frac{n+2}{2} \frac{r_0^n}{r^n} \right) \sum_{i=1}^{p} f_{ii}}{n+1} - 2c_{vr} + \frac{r_0^n}{r^n} c_{vv} . \tag{5.2.29}$$

Again these are regular at the horizon for all choices of the integration constants. Note that f_{rj} does not appear in Einstein's equations to first order in ϵ and corresponds to a gauge mode. This, and the integration constants, will be fixed shortly.

At this stage, for any hydrodynamic perturbation that solves the equations (5.2.21), we have managed to construct a perturbed metric that is regular at the horizon. Next we must ensure that the solution remains asymptotically flat. Transforming to Schwarzschild-like coordinates using (5.2.16), we require that

$$g_{ab} = \eta_{ab} + O(r^{-n}) . \tag{5.2.30}$$

For the other metric components, we find that $g_{rr} = 1 + O(r^{-n})$, $g_{ri} = O(r^{-n})$, and $g_{tr} = O(r^{-n+1})$ when $n > 1$ ($g_{tr} = O(\log r / r)$ when $n = 1$), are enough to obtain a finite stress tensor. Recall also that all the metric components involving angular coordinates of S^{n+1} are unaltered.

Omitting details, we find that the conditions on g_{ij} and g_{tj} fix

$$c_{ij} = c_{vj}^{(2)} = 0 . \tag{5.2.31}$$

In addition, the effect of $c_{vj}^{(1)}$ in g_{tj} amounts to a global shift in the velocity field along the spatial directions of the brane, so in order to remain in a local rest frame we set

$$c_{vj}^{(1)} = 0 . \tag{5.2.32}$$

Furthermore, if we perform the change

$$t \to t \left(1 - \epsilon c_{vr} \right) , \tag{5.2.33}$$

then $c_{vv} - 2c_{vr}$ results in a global shift in the temperature, which we eliminate by choosing

$$c_{vv} = 2c_{vr} . \tag{5.2.34}$$

36

Asymptotic flatness in g_{tr} imposes a choice for c_{vr} that singles out the slower fall-off of $n = 1$,

$$c_{vr} = -\partial_t r_0 \quad \text{for } n = 1 , \qquad c_{vr} = 0 \quad \text{for } n > 1 \qquad (5.2.35)$$

(note that the values of $\partial_t r_0$ and $\partial_v r_0$ at $\sigma^a = 0$ are equal).

Asymptotic flatness in these coordinates is a little delicate when $n = 1$ due to its slower fall-off, and to make it manifest we take an f_{rj} gauge diverging at infinity. This is not necessary when $n > 1$ (and neither choice affects the calculation of the stress tensor). Thus we set

$$f_{rj} = -\partial_j r_0 \log \frac{r}{r_0} \quad \text{for } n = 1 , \qquad f_{rj} = 0 \quad \text{for } n > 1 . \qquad (5.2.36)$$

Summarizing, we obtain

$$g_{ij} = \delta_{ij} + \epsilon r_0 \frac{2\partial_{(i} u_{j)}}{n} \log f , \qquad (5.2.37)$$

$$g_{tj} = -\epsilon \frac{r_0^n}{r^n} \sigma^a \partial_a u_j , \qquad (5.2.38)$$

$$g_{tr} = \epsilon \frac{\partial_t r_0}{f} \left(\left(\frac{r_0^n}{r^n} - \frac{f}{n} \right) \log f - \frac{r_0^n}{r^n} \left(n \frac{r_*}{r_0} + 1 \right) \right) - \epsilon c_{vr} , \qquad (5.2.39)$$

$$g_{rj} = \epsilon f_{rj}(r) + \epsilon \frac{\partial_j r_0}{r_0} \frac{r_* - r}{f} , \qquad (5.2.40)$$

$$g_{rr} = f^{-1} + \epsilon f^{-2} \left(\frac{n r_0^{n-1} \sigma^a \partial_a r_0}{r^n} + \frac{r_0^n \partial_t r_0}{r^n} (\log f - 2) \right) , \qquad (5.2.41)$$

$$g_{tt} = -f + \epsilon \left(\frac{n r_0^{n-1} \sigma^a \partial_a r_0}{r^n} + \partial_t r_0 \log f \left(\frac{r_0^n}{r^n} - \frac{2}{n} f \right) \right) , \qquad (5.2.42)$$

(σ^a correspond to Schwarzschild coordinates here, so $\sigma^0 = t$). This is the complete solution for the black brane metric that corresponds to a hydrodynamic perturbation that solves the equations (5.2.21) expanded around the origin of the local rest frame, $\sigma^a = 0$.

5.2.3 Viscous stress tensor

We are now ready to compute the quasilocal stress tensor (5.2.2). The renormalization via background subtraction is simple and appropriate, since our metrics are infinitesimally close to the uniform black p-brane and their asymptotic boundaries can always be embedded in flat spacetime. Straightforward calculations give

$$T_{ij} = \frac{\Omega_{n+1}}{16\pi G} \left(-\delta_{ij} (r_0 + \epsilon \sigma^a \partial_a r_0)^n - \epsilon r_0^{n+1} \left[\left(2\partial_{(i} u_{j)} - \frac{2}{p} \delta_{ij} \partial^\ell u_\ell \right) + 2 \left(\frac{1}{p} + \frac{1}{n+1} \right) \delta_{ij} \partial^\ell u_\ell \right] \right) ,$$

$$T_{tt} = \frac{\Omega_{n+1}}{16\pi G} (n+1) (r_0 + \epsilon \sigma^a \partial_a r_0)^n , \qquad (5.2.43)$$

$$T_{tj} = -\frac{\Omega_{n+1} r_0^n}{16\pi G} \epsilon n \sigma^a \partial_a u_j ,$$

37

which are valid up to $O(\epsilon^2)$. One can easily check that the hydrodynamic equations $\partial_a T^{ab} = 0$ are indeed equivalent to the constraint equations (5.2.21).

Write now this stress tensor in the form

$$T_{ab} = \rho u_a u_b + P P_{ab} - \zeta \theta P_{ab} - 2\eta \sigma_{ab} + O(\partial^2) \tag{5.2.44}$$

where the expansion and shear of the velocity congruence are

$$\theta = \partial_a u^a \,, \qquad \sigma_{ab} = P_a^{\ c} \left(\partial_{(c} u_{d)} - \frac{1}{p} P_{cd} \right) P^d_{\ b} \,. \tag{5.2.45}$$

The component T_{tt} in (5.2.43) determines the energy density, and requiring that the equation of state (5.1.1) holds locally uniquely identifies the pressure. Then we can write

$$T_{ij} = P\delta_{ij} - \epsilon\eta \left(2\partial_{(i} u_{j)} - \frac{2}{p}\delta_{ij}\partial^\ell u_\ell \right) - \epsilon\zeta\delta_{ij}\partial^\ell u_\ell \tag{5.2.46}$$

with

$$\eta = \frac{\Omega_{n+1}}{16\pi G} r_0^{n+1} \,, \qquad \zeta = \frac{\Omega_{n+1}}{8\pi G} r_0^{n+1} \left(\frac{1}{p} + \frac{1}{n+1} \right) \,. \tag{5.2.47}$$

Using (5.1.4) and (5.2.8) these can be rewritten as in (5.1.3).

5.3 Damped unstable sound waves and the Gregory-Laflamme instability

Our analysis in the previous section applies to generic long-wavelength perturbations of arbitrarily large amplitude. Let us now consider small perturbations of a static fluid of the form

$$\rho \to \rho + \delta\rho \,, \qquad P \to P + c_s^2\delta\rho \,, \qquad u^a = (1, 0, \dots) \to (1, \delta u^i) \,, \tag{5.3.1}$$

where c_s is the speed of sound, and with

$$\delta\rho(t, \sigma^i) = \delta\rho\, e^{i\omega t + i k_j \sigma^j} \,, \qquad \delta u^i(t, \sigma^i) = \delta u^i\, e^{i\omega t + i k_j \sigma^j} \,. \tag{5.3.2}$$

We substitute these in the viscous fluid equations and linearize in the amplitudes $\delta\rho$ and δu^i, to find

$$\omega\delta\rho + (\rho + P)k_i\delta u^i + O(k^3) = 0 \tag{5.3.3}$$

$$i\omega(\rho + P)\delta u^j + i c_s^2 k^j \delta\rho + \eta k^2 \delta u^j + k^j \left(\left(1 - \frac{2}{p}\right)\eta + \zeta \right) k_l \delta u^l + O(k^3) = 0 \tag{5.3.4}$$

38

Applying our results above, any solution to these equations can be used to obtain an explicit black brane solution with a small, long-wavelength fluctuation of r_0 and u^a. If we eliminate $\delta\rho$ we find that non-trivial sound waves require

$$\omega - c_s^2 \frac{k^2}{\omega} - i\frac{k^2}{Ts}\left(2\left(1 - \frac{1}{p}\right)\eta + \zeta\right) + O(k^3) = 0\,, \qquad (5.3.5)$$

where $k = \sqrt{k_i k_i}$ and we have used the Gibbs-Duhem relation $\rho + P = Ts$. This equation determines the dispersion relation $\omega(k)$. For a stable fluid with $c_s^2 > 0$, viscosity adds a small imaginary part to the frequency, which becomes complex and describes damped sound oscillations. Instead our effective fluid has imaginary sound-speed, eq. (5.1.4), so ω is purely imaginary: sound waves are unstable. Writing

$$\omega = -i\Omega \qquad (5.3.6)$$

we solve (5.3.5) to find

$$\Omega = \sqrt{-c_s^2}\,k - \left(\left(1 - \frac{1}{p}\right)\frac{\eta}{s} + \frac{\zeta}{2s}\right)\frac{k^2}{T} + O(k^3)\,. \qquad (5.3.7)$$

For the specific black p-brane fluid this yields the dispersion relation (5.1.5). The connection between these unstable sound waves and the Gregory-Laflamme instability was pointed out at the perfect fluid level (*i.e.*, Ω linear in k) in [27], and we have discussed it in the introduction.[5]

Figures 5.1 and 5.2 show that our approximation (5.1.5) improves as n grows. In order to see how this might be justified, let us first rewrite the dispersion relation (5.1.5) in terms of the temperature T instead of r_0,

$$\Omega = \frac{k}{\sqrt{n+1}}\left(1 - \frac{n+2}{\sqrt{n+1}}\frac{k}{4\pi T} + O(k^2/T^2)\right)\,. \qquad (5.3.8)$$

In principle, at any given n, both quantities r_0 and T^{-1} define length scales that are parametrically equivalent. But if we vary n and allow it to take large values, then r_0 and $T^{-1} \sim r_0/n$ can differ greatly. We propose that in this case, T^{-1}, and not r_0, is the length scale that limits the validity of the fluid approximation, so the appropriate expansion variable for large n is k/T and not kr_0. This may actually be natural since from the fluid point of view T has a clearer physical meaning than r_0. In effect, we are proposing that when $n \gg 1$ it is more accurate to view the effective theory as describing very *hot* black branes, rather than very *thin* ones.

---

[5]Observe that the result (5.1.5) is independent of p. That this must be the case is clear from the outset in the GL analysis and also in our analysis of the Einstein equations.

The point of this exercise is that for large n the maximum values over which Ω and k in (5.3.8) range are $(k/T)|_{\max} \sim 1/\sqrt{n}$ and $(\Omega/T)|_{\max} \sim 1/n$. So as n grows the frequency and wavenumber of unstable modes extend over a smaller range of k/T and Ω/T. This strongly suggests that hydrodynamics can capture more accurately the dynamics of GL modes when the number of dimensions becomes very large.[6] More precisely, if we write the corrections inside the brackets in (5.3.8) in the form $\sum_{j\geq 2} a_j (k/T)^j$, and assume that the n-dependence of the coefficients a_j is such that $a_j n^{-j/2} \to 0$ as $n \to \infty$, then the expansion in k/T, *i.e.,* the hydrodynamic derivative expansion, becomes a better approximation over a larger portion of the curves $\Omega(k)$.

This is a relatively mild-looking assumption on the n-dependence of the higher-order coefficients in the expansion in k/T,[7] and in particular is satisfied if the $a_{j \geq 2}$ remain finite as $n \to \infty$. But since we have not computed higher-derivative transport coefficients then, within our perturbative framework, we cannot prove its validity. However, since the numerical data appear to strongly support it, we conjecture that the truncation of the dispersion relation up to k^2-terms captures the complete dispersion relation at large n. More precisely, if we define a rescaled frequency and wavenumber,

$$\tilde{\Omega} = n\Omega\,, \qquad \tilde{k} = \sqrt{n}k \tag{5.3.9}$$

that remain finite as $n \to \infty$, then we propose that

$$\tilde{\Omega} = \tilde{k}\left(1 - \frac{\tilde{k}}{4\pi T}\right) \tag{5.3.10}$$

is the exact limiting relation valid for all wavenumbers $0 \leq \tilde{k} \leq 4\pi T$.

Note that the truncation of $\Omega(k)$ in (5.3.8) appears to capture the zero-mode with $\Omega = 0$ at a finite $k = k_{GL}$. This is quite remarkable, since the viscous fluid equation (5.3.5) does not admit any zero-mode solution. The comparison with numerical data in figure 5.2 shows that the quantitative result for k_{GL}, although poor for small n, becomes excellent for large n. Further evidence for the validity of our proposal comes from the analytical value of the GL zero mode in the limit $n \to \infty$ [40]

$$k_{GL} \to \frac{4\pi T}{\sqrt{n}}\,. \tag{5.3.11}$$

This is the same as the limiting value for the zero-mode 'predicted' by (5.3.9), (5.3.10).[8]

---

[6]This is similar in spirit, although not precisely equal, to the proposal in [39] that in the limit of large number of dimensions black holes are accurately described by fluid mechanics.

[7]Which, crucially, is not satisfied by the coefficient of the linear term inside the brackets in (5.3.8).

[8]The relative difference between the results for k_{GL} from the large-n subleading correction computed in [41] and from (5.1.5) is equal to $1/n$. This is precisely the size of the discrepancy observed in fig. 5.2.

Presumably, by effecting the scaling (5.3.9) in the full linearized perturbation equations of the GL problem one may prove (or possibly disprove) equation (5.3.10).

5.4 Discussion

Our analysis of the GL instability must not be confused with recent studies where a connection to the Rayleigh-Plateau instability of fluid tubes is made. In the latter approach, following a suggestion in [42], refs. [39, 43] related a d-dimensional black string in a Scherk-Schwarz compactification of Anti-deSitter space to a $d-2$-dimensional fluid tube with a boundary with surface tension (see [44]). The Rayleigh-Plateau instability of the fluid tube arises from the competition between surface tension and bulk pressure. In contrast, our effective fluid does not have any boundaries so the instability is not of the Rayleigh-Plateau type, but rather one in the sound modes. Also note that our calculations in sec. 5.2 yield explicit black brane solutions to the Einstein equations (in vacuum) in a derivative expansion, something that, although expected to be possible in principle, at present cannot be realized for the fluid solutions in [39, 43].

We stress that our analysis is not a 'dual' solution of the GL instability problem: we have investigated the same perturbation problem as in [34] and explicitly solved it in closed analytic form in a derivative expansion. Since our approach does not require the perturbations to be small, it may even be used to study the non-linear evolution of the GL instability.

One of our motivations has been to show explicitly how the effective theory of blackfolds of [27] can be systematically developed as a derivative expansion of the Einstein equations. Although we have done it only for the intrinsic aspects of blackfold dynamics, we have been able to: (i) derive in detail, starting from the 'microscopic' (full Einstein) theory, the lowest-order blackfold formalism that ref. [27] had developed following general principles; (ii) prove that the first corrections to the lowest-order formalism can be computed and result in perturbations of the black brane that preserve regularity of the horizon. The viscosity coefficients are determined precisely from this condition.

In general, the worldvolume of a blackfold is dynamical and can be curved. Our calculations in this paper can be regarded as being valid for fluid perturbations with a wavelength that, while longer than T^{-1}, is much shorter than the typical curvature radius R of the blackfold worldvolume. In this case, the intrinsic and extrinsic dynamics decouple. Thus, for a curved blackfold our results for the GL instability are valid at most up to wavelengths smaller than R. At longer wavelengths the hydrodynamics of the effective fluid is fully coupled to the elastic dynamics of the worldvolume. For

instance this is case for perturbations of thin black rings with wavelength comparable to the ring radius. These lie beyond the range of applicability of our results.

It should be quite interesting to extend our analysis to include the extrinsic aspects of the blackfold. To do this, one first allows the worldvolume metric where the fluid lives to be a curved background, with an extrinsic curvature radius much larger than T^{-1}. This curvature acts as an external force on the fluid [27]. In the derivative expansion, the stress tensor will in general contain, besides the viscosities, higher-derivative coefficients that multiply derivatives of the worldvolume metric. These coefficients will be determined by demanding horizon regularity of a perturbation that curves the asymptotic geometry. Perturbations of this kind have been studied for certain illustrative examples in [45, 46, 29] in stationary situations that do not involve viscous dissipation. Thus it may be possible to extract the extrinsic pressure coefficients in the stress tensor.

In the AdS context, the external force on the fluid from a worldvolume curvature has been studied in [47]. However, in that case the worldvolume geometry is regarded as a fixed, non-dynamical background. Instead, in the blackfold context this geometry is dynamical. A solution of the forced fluid equations will backreact on the background spacetime where the blackfold lives, and thus modify the worldvolume geometry. Therefore for a generic, curved blackfold the explicit construction of perturbative metrics becomes rather more complicated than in the fluid/AdS-gravity correspondence.

Chapter 6

Self-similar critical geometries at horizon intersections and mergers

6.1 Introduction

As was said in chapter 2 and chapter 4, black holes in higher dimensions exhibit a pattern of phases much more intricate than the simple situation that uniqueness theorems impose in four dimensions. Unraveling the structure of this phase space is a problem in which, despite the steady progress in recent years, there remain important open issues. In particular, the topology-changing transitions in the space of solutions at which horizons split or merge involve all the non-linearity of Einstein's theory and lie far from the regimes where analytic perturbative techniques of the type developed in [28, 27] would apply. Numerical methods, while very valuable, face the problem that the geometries that effect the change in topology involve curvature singularities.

The most studied example of this phenomenon[1] is the black hole-black string transition in Kaluza-Klein compactified spacetimes [48], which we already explained, in some details, in chapter 4. The uniform string phase branches into a non-uniform black string phase [49] whose non-uniformity grows until a cycle along the horizon of the string pinches down to zero size. The same pinched-off phase can be approached from black holes localized in the KK circle, where the size of the black hole grows until the two opposite poles of the horizon come into contact with each other along the circle [50] (see ref. [51] for the state of the art in solutions on both sides of the transition). Early in these studies, ref. [52] emphasized that the pinched-off solution plays the role of a critical point in phase space and argued that some of its properties, in particular the local geometry near the singular pinch-off region, should be determined

---

[1]In this chapter we are concerned only with evolution in the phase space of stationary black hole solutions, not with time evolution in dynamical mergers of horizons.

by general symmetry considerations. Specifically, it was proposed, using an argument that we summarized in fig. 4.1, that this geometry (after Wick-rotation to Euclidean time) is locally modelled by a self-similar cone over $S^2 \times S^{D-3}$. The transition between phases is analogous to the 'conifold transition', where the critical cone geometry can be smoothed in two ways, each one leading to one of the phases at each side of the transition.

Ref. [52] could present in exact form only the local conical geometry asymptotically close to the pinch-off point. The details of how, and even whether, this conical region extends to a full critical solution in the KK circle remained open. Moreover, the non-singular geometries that approach the critical solution are only known perturbatively or numerically (see [53, 54] and other works cited above). The aim of this chapter is to, first, present an exact example of a horizon-merger transition that provides strong analytic evidence for the conifold-type picture, and second, to argue for the universality of this picture among wide classes of topology-changing transitions involving higher-dimensional black hole phases.

To this end, in section 6.2 we present a complete, exact family of geometries that approach a merger of horizons, and we give explicitly the critical solution at the merger. The system describes the meeting of the horizon of a black hole with a cosmological deSitter horizon in any $D \geq 6$, with the black hole sufficiently distorted away from spherical symmetry that it intersects the deSitter horizon along a circle, and not on all points on the horizon. This study confirms that the critical solution near the pinch-off is locally a self-similar cone with the geometry anticipated in [52]. Section 6.3 is an attempt to find the geometry after the horizons have merged into a single one. Unfortunately, the result is only partially successful since the solution presents some pathologies.

In section 6.4 we describe the critical geometries at the merger point in other important instances — here we do not have a description of the approach to the merger transition, but we can always identify the local model for the critical geometries. Refs. [45, 55] (following [56]) have proposed the following picture for a specific class of topology-changing transitions: a black ring of horizon topology $S^1 \times S^{D-3}$ in $D \geq 6$ becomes, as its spin decreases, fat enough that its hole closes up. Coming from the other side of the transition, the same phase is reached when a pinched rotating black hole pinches off to a singularity at its axis of rotation. In this chapter we describe the local conical geometry that controls this transition. We also extend the analysis to similar transitions that involve black holes with horizon topology $S^p \times S^{D-p-2}$, with $p \geq 1$ [28, 29]. We find the critical conical geometries that appear when the round S^p closes off and the critical solution connects to a black hole of spherical topology. Other
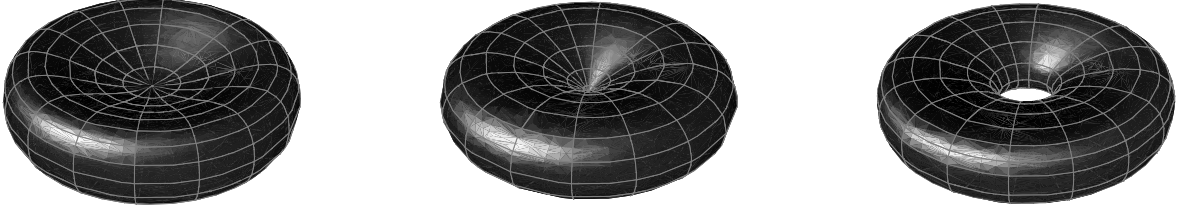
Figure 6.1: Black ring pinch in $D \geq 6$. The pictures are only illustrative of expected solutions that are yet to be constructed. In sec. 6.4 we describe the critical geometry near the self-similar pinch-off point.
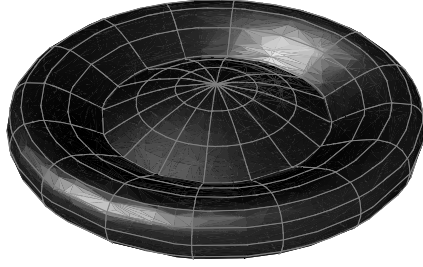

Figure 6.2: Circular pinch in the transition involving a black Saturn in $D \geq 6$.

conical geometries, for instance those that appear at the merger of a black ring and a black hole, or two black rings, are easily obtained too.

An interesting, perhaps unexpected, consequence of our analysis is that the critical conical geometries appear not only when horizons merge, but more generally when they just intersect. To understand the distinction, note that if there is an actual transition in which two separate horizons merge to form one horizon, the surface gravities (*i.e.,* temperatures) of the two horizons must approach the same value at the critical solution. However, we find exact critical solutions in which the two horizons have different surface gravities. These horizons can approach and touch each other locally, *i.e.,* intersect, over a singularity, but they cannot merge to form a single, connected horizon over which the temperature must be uniform. Such intersection geometries correspond to endpoints of trajectories in the space of solutions, and not to topology-changing transitions. We find that they also take the form of self-similar cones, but their base is not a homogeneous space (a direct product of round spheres) but an inhomogeneous one (a warped product).

45

Caveat emptor, evolution in the space of black hole solutions, as studied in this chapter, occurs along geometries that can be quite different than in dynamical evolution in time, as the example of the black string/black hole transition shows [57]. Presumably this is also the case in the instances we discuss here.

6.2 Intersection of black hole and deSitter horizons

The so-called D-dimensional Kerr-deSitter solution for a rotating black hole in deSitter space with a single rotation, as found in [58] but with a shift $\phi \to \phi + at/L^2$, is

$$ds^2 = -\frac{\Delta_r}{\rho^2 \Xi^2} \left(\Delta_\theta dt - a \sin^2 \theta d\phi \right)^2 + \rho^2 \left(\frac{dr^2}{\Delta_r} + \frac{d\theta^2}{\Delta_\theta} \right)$$
$$+ \frac{\Delta_\theta \sin^2 \theta}{\rho^2 \Xi^2} \left((r^2 + a^2)d\phi - a \left(1 - \frac{r^2}{L^2} \right) dt \right)^2 + r^2 \cos^2 \theta d\Omega^2_{(D-4)} \quad (6.2.1)$$

with

$$\rho^2 = r^2 + a^2 \cos^2 \theta \,, \tag{6.2.2}$$

$$\Delta_r = (r^2 + a^2) \left(1 - \frac{r^2}{L^2} \right) - \frac{2M}{r^{D-5}} \,, \tag{6.2.3}$$

$$\Delta_\theta = 1 + \frac{a^2}{L^2} \cos^2 \theta \,, \tag{6.2.4}$$

$$\Xi = 1 + \frac{a^2}{L^2} \,, \tag{6.2.5}$$

and

$$0 \leq \theta \leq \frac{\pi}{2} \,, \qquad 0 \leq \phi \leq 2\pi \,. \tag{6.2.6}$$

The metric satisfies $R_{\mu\nu} = (D-1)L^{-2} g_{\mu\nu}$. When $M = 0$ this is deSitter spacetime in 'ellipsoidal coordinates'. When M is non-zero and positive, there is a range of values of M and a for which the function Δ_r has two real positive roots that correspond to the black hole and cosmological horizons. With non-zero rotation $a \neq 0$, both horizons are distorted away from spherical symmetry. For reasons that will become apparent, we only consider $D \geq 6$.

6.2.1 Horizon intersection

We want to take a limit in which the black hole grows and its horizon touches the cosmological horizon, in such a way that this occurs not uniformly over all of the horizon, but only along the 'equator' at $\theta = \pi/2$, as illustrated in fig. 6.3. There is an intuitive reason why this should be possible in $D \geq 6$: in these dimensions, Myers-Perry
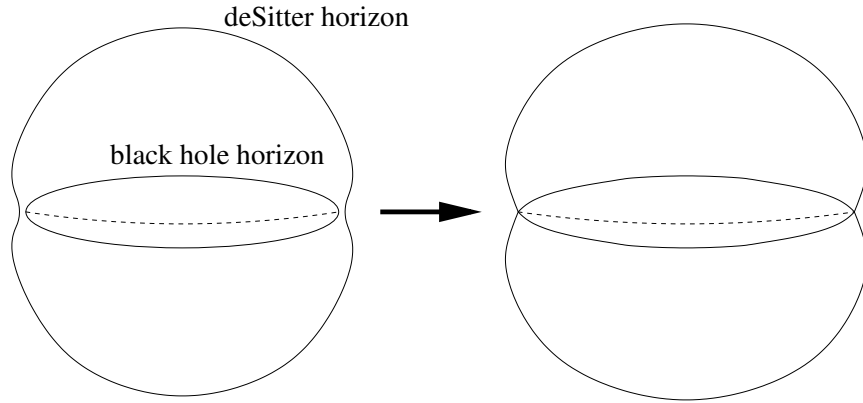
Figure 6.3: Sketch of black hole-deSitter horizons in the approach to the solution in which the black hole touches the deSitter (cosmological) horizon along its equator. Only in $D \geq 6$ does the black hole admit a large enough distortion away from spherical symmetry to allow this type of configuration.

black holes rotating along one plane can become very flat and thin, effectively like disks of a black membrane [56]. The blackfold approach of [28, 27] allows to construct a *static* configuration in which this disk extends along a plane and touches the deSitter horizon. This blackfold construction is easy to perform and gives an approximate solution for the intersecting-horizon configuration. However, we will not give its details since we can obtain the complete exact solution that it is an approximation to.

The appropriate limit of (6.2.1) is

$$a, M \to \infty \qquad (6.2.7)$$

keeping fixed

$$\mu = \frac{2M}{a^2} \, . \qquad (6.2.8)$$

Even if we are taking the rotation parameter a to be very large, this does not mean that the black hole rotates very rapidly relative to the cosmological horizon. By taking M large we are also making the black hole size grow. The relative drag between the two horizons increases and as a consequence they approach corotation, with the relative angular velocity decreasing. Eventually, when the black hole touches the deSitter horizon, the configuration becomes manifestly static with our choice of coordinates. However, as we shall see presently, since the distortion away from spherical symmetry remains in the limit, the horizons touch only along the equator.

Taking the above limit in (6.2.1), we find

$$ds^2 = L^2(d\theta^2 + \sin^2\theta d\phi^2)$$

$$+ \cos^2\theta \left(- \left(1 - \frac{\mu}{r^{D-5}} - \frac{r^2}{L^2} \right) dt^2 + \frac{dr^2}{1 - \frac{\mu}{r^{D-5}} - \frac{r^2}{L^2}} + r^2 d\Omega^2_{(D-4)} \right)$$

$$= L^2 \left(d\theta^2 + \sin^2\theta d\phi^2 \right) + \cos^2\theta \, ds^2(\text{Schw-dS}_{D-2}), \qquad (6.2.9)$$

where Schw-dS$_{D-2}$ denotes the Schwarzschild-deSitter geometry in $D-2$ dimensions. When $\mu = 0$ this factor becomes $(D-2)$-dimensional deSitter (dS$_{D-2}$) and the whole geometry is dS$_D$ spacetime of radius L. The singularity at $\theta = \pi/2$ in this metric is just a coordinate artifact. The cosmological horizon at $r = L$ has the usual geometry of a round S^{D-2}.

Our actual interest is in the solutions with $\mu \neq 0$. Then the singularity at $\theta = \pi/2$ is a true one where the curvature diverges. Setting $\theta - \pi/2 = z/L$, then near $z = 0$ the geometry asymptotically becomes

$$ds^2 \to dz^2 + L^2 d\phi^2 + \frac{z^2}{L^2} ds^2(\text{Schw-dS}_{D-2}). \qquad (6.2.10)$$

This has the form of a cone over Schw-dS$_{D-2}$, spread along the circle generated by ϕ.

Before we took the limit, the solution (6.2.1) in the parameter range of interest described two separate horizons, black hole and cosmological. In the limiting solution, these are still present. The equation

$$\frac{r^2}{L^2} + \frac{\mu}{r^{D-5}} = 1 \qquad (6.2.11)$$

with

$$0 < \frac{\mu}{L^{D-5}} < \frac{2}{D-5} \left(\frac{D-5}{D-3} \right)^{\frac{D-3}{2}} \qquad (6.2.12)$$

has two real positive roots for r, for the black hole and cosmological horizons in the Schw-dS$_{D-2}$ sub-spacetime. These are the limits of the black hole and cosmological horizons of the original solution (6.2.1) in D dimensions. In (6.2.9) these two horizons come to touch each other along the circle $\theta = \pi/2$.

The continuously self-similar structure of a cone around this intersection point is apparent in (6.2.10). If we analytically continue to Euclidean time τ, then the (τ, r) part of the Schw-dS$_{D-2}$ geometry describes a two-sphere, generically with a conical defect (of codimension 1) at either the cosmological or black hole horizons since their temperatures are not the same for generic values of μ/L^{D-5}. Except for this defect the Euclidean geometry of Schw-dS$_{D-2}$ is a warped product of $S^2_{(\tau,r)}$ and S^{D-4}. So the Euclidean continuation of (6.2.10) is a cone over this warped $S^2 \times S^{D-4}$, times the ϕ

circle. This cone is essentially the local model for the critical geometry that [52] had proposed.

Note, however, that what we have found is a more general cone than in [52]. In (6.2.9) the temperatures of the black hole and of the cosmological horizons need not be the same. For instance, in configurations where the black hole has the shape of a very thin pancake, which occur when $\mu \ll L^{D-5}$, the black hole temperature is clearly much higher than the temperature of the cosmological horizon.[2]

When their temperatures are different, the two horizons can approach each other and *intersect*, but not evolve beyond the intersection to *merge* and form a single, connected horizon. Since the temperature over the latter must be uniform, a merger requires that the temperatures of the two horizons approach the same value at the intersection. Ref. [52] focused on merger transitions, but we have seen that the appearance of self-similar conical geometries is a more general feature of intersections of horizons, even when they cannot merge. For the Lorentzian solutions the difference in temperatures does not imply any pathology, so it is natural to consider these configurations as well.

The parameter μ in the critical geometry (6.2.9) can be adjusted so that the two horizons have the same surface gravity. In fact it is possible to consider not only this solution, but an entire subfamily of solutions of (6.2.1) in which the two separate horizons, black hole and cosmological, have the same surface gravity even away from the critical merger geometry. This subfamily of solutions describes a rotating black hole with the same temperature as the cosmological horizon, *i.e.,* a 'rotating Nariai' solution, and is of some interest in itself, so we describe it next.

6.2.2 Isothermal solutions

The limit of the solutions (6.2.1) where the two separate horizons have equal temperatures, or surface gravities, is defined in appendix A. The mass and the radial coordinate are fixed to values $M = M_0$ and $r = r_0$ that depend on the rotation parameter a. Using for simplicity units where $L = 1$, the metric that results is

$$ds^2 = C\rho_0^2(-\sin^2\chi d\tilde{t}^2 + d\chi^2) + \frac{\rho_0^2}{\Delta_\theta}d\theta^2$$
$$+ \frac{\Delta_\theta \sin^2\theta}{\rho_0^2 \Xi^2}\left((r_0^2 + a^2)d\tilde{\phi} - 2Cr_0a\Xi\cos\chi d\tilde{t}\right)^2 + r_0^2\cos^2\theta d\Omega_{(D-4)}^2 . \quad (6.2.13)$$

---

[2]The blackfold method reproduces these configurations to leading order in $\mu/L^{D-5} \ll 1$. In the exact solutions one can take a limit to focus on the region very close to the axis $\theta = 0$ and recover the geometry of a black 2-brane of thickness much smaller than L.

where
$$\rho_0^2 = r_0^2 + a^2 \cos^2 \theta \,, \tag{6.2.14}$$

and Δ_θ, Ξ as in (6.2.4), (6.2.5) (with $L = 1$) and
$$0 \le \chi \le \pi \,, \qquad 0 \le \theta \le \frac{\pi}{2} \,, \qquad 0 \le \tilde{\phi} \le 2\pi \,. \tag{6.2.15}$$

The constants r_0 and C are determined in terms of a by
$$a^2 = r_0^2 \frac{D - 3 - (D - 1)r_0^2}{(D - 3)r_0^2 - (D - 5)} \tag{6.2.16}$$

and
$$C = \frac{(D - 3)r_0^2 - (D - 5)}{(D - 1)(D - 3)r_0^4 - 2(D - 5)(D - 1)r_0^2 + (D - 5)(D - 3)} \,. \tag{6.2.17}$$

Actually, we could take the only parameter in the solution to be r_0 instead of a, since they are related in one-to-one manner in the range of interest, which is
$$0 \le a \le \infty \,, \qquad \frac{D - 5}{D - 3} \le r_0^2 \le \frac{D - 3}{D - 1} \tag{6.2.18}$$

(note this implies $r_0^2 < 1$).

In going from (6.2.1) to (6.2.13), the cohomogeneity of the geometry has been reduced from two to one, the only non-trivial dependence being now on θ. It is manifest that the surface gravities at the two horizons, at $\chi = 0$ and $\chi = \pi$, are equal. However, there is a relative angular velocity between them,
$$\Omega_{rel} = \frac{4C r_0 a \Xi}{r_0^2 + a^2} \,. \tag{6.2.19}$$

For a merger of the two horizons to be possible, this relative motion between them must disappear at the critical solution.

In the conventional static limit $a \to 0$, where $r_0^2 \to (D - 3)/(D - 1)$, eq. (6.2.13) becomes the Nariai limit of Schw-dS$_D$, namely the direct product geometry
$$ds^2 \xrightarrow{a \to 0} \frac{1}{D - 1}(-\sin^2 \chi d\tilde{t}^2 + d\chi^2) + \frac{D - 3}{D - 1} d\Omega^2_{(D-2)} \tag{6.2.20}$$

which Wick-rotates to $S^2 \times S^{D-2}$. In this solution, and in all the solutions with finite a, the two horizons remain separate.

The limit that we are interested in, where the two horizons touch at the equator $\theta = \pi/2$, lies at $a \to \infty$, with $r_0^2 \to (D - 5)/(D - 3)$. Then $\Omega_{rel} \to 0$ (as we had already observed in the previous section) and
$$ds^2 \xrightarrow{a \to \infty} \frac{1}{D - 3} \cos^2 \theta (-\sin^2 \chi d\tilde{t}^2 + d\chi^2) + d\theta^2 + \sin^2 \theta d\tilde{\phi}^2 + \frac{D - 5}{D - 3} \cos^2 \theta d\Omega^2_{(D-2)} \,. \tag{6.2.21}$$

50

This is indeed the same geometry that results if we take the Nariai limit of the Schw-dS$_{D-2}$ geometry inside (6.2.9). We have obtained it here along a particular one-parameter subfamily of the solutions (6.2.1).

In the region close to the intersection of horizons, with small $\theta - \pi/2 = z/L$, the geometry (6.2.21) becomes, after rotation to Euclidean time (and restoring L),

$$ds^2 \to dz^2 + L^2 d\tilde{\phi}^2 + \frac{z^2}{D-3} \left(d\Omega_{(2)}^2 + (D-5)d\Omega_{(D-4)}^2 \right) , \qquad (6.2.22)$$

which is exactly the kind of double-cone geometry predicted by the arguments in [52].

We have studied the solutions in which the initial black hole rotates along a single plane, but it is straightforward to extend this to the general solutions with rotation in an arbitrary number of planes and then obtain intersections along odd-spheres instead of circles. Appendix B explains this construction.

6.3   Merged solution

It is natural now to look for an exact solution for the geometry after the two horizons have merged into a single one. Here we describe our attempt at finding this solution. In contrast to the pre-merger solution of the previous section, the merged solution that we find is not entirely satisfactory — its Lorentzian section is complex, and it has a naked singularity. It is unclear to us whether this is a deficiency somehow intrinsic to the (cosmological) set up that we are considering, or whether there is another solution for the merged configuration. Readers not interested in the details can safely jump to section 6.4.

One might expect, by analyticity in the space of solutions, that the solution after the black hole and cosmological horizons have merged should be in the same family as (6.2.13), but in a different parameter range than before the merger — *i.e.,* in the merged solution the parameter a extends beyond the range we have been considering in sec. 6.2.2. Actually, we will consider not only (6.2.13), or the initial Kerr-dS solution (6.2.1), but the Kerr-NUT-dS family. This is the largest known family of solutions that appear appropriate for this task. As in section 6.2, away from the critical solution we consider the Lorentzian section of the geometries.

It is useful to first identify the main properties that the solution must possess. First, the family of solutions should obviously have a limit to the critical geometry (6.2.21).

Second, from the general picture of the conifold-type transition, in the merged solution there should be a 'Lorentzian two-sphere' (like the one that $\tilde{t}$ and χ describe in (6.2.21)) that is contractible to zero, and a S^{D-4} that is not. Observe that this, and
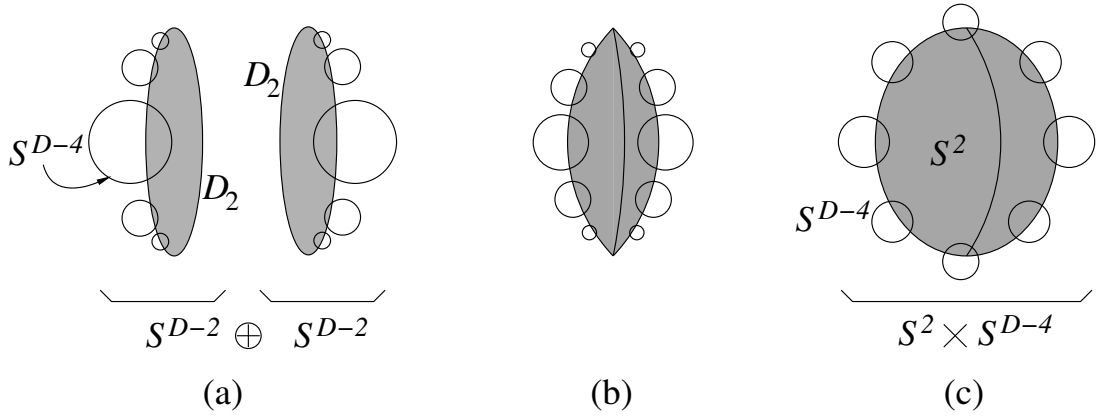
Figure 6.4: Horizon geometry in (a) the black hole-deSitter phase; (b) critical solution; (c) merged solution.

the first condition, rule out the simple possibility that when the two horizons merge we recover dS$_D$.

Finally, we can easily determine the topology of the spatial sections of the horizon. As illustrated in figure 6.4, before the merger the horizon is the sum of two S^{D-2}. Each of these spheres can be viewed as the result of fibering the (topological) disk D_2, parametrized by (θ, ϕ), with spheres S^{D-4} whose size goes to zero at the boundary of the disk at $\theta = \pi/2$. In the critical geometry, the two disks meet at their edges: they form a topological S^2. The spheres S^{D-4} fiber over this S^2, with their sizes shrinking to zero at the circle where the two disks meet: this is the horizon of the critical solution. When the two horizons merge to form a single one, the S^{D-4} do not shrink to zero anywhere, so the horizon of the merged solution has the topology $S^2 \times S^{D-4}$.[3]

Consider now the Kerr-NUT-dS solution in D-dimensions [59], in units of $L = 1$,

$$ds^2 = \rho^2 \left(\frac{dr^2}{\Delta_r} + \frac{du^2}{\Delta_u} \right) - \frac{\Delta_r}{\rho^2 \Xi^2} \left((1 + a^2 u^2) dt - a(1 - u^2) d\phi \right)^2$$
$$+ \frac{\Delta_u}{\rho^2 \Xi^2} \left((r^2 + a^2) d\phi - a(1 - r^2) dt \right)^2 + r^2 u^2 d\Omega^2_{(D-4)} \tag{6.3.1}$$

with Δ_r and Ξ as in (6.2.3), (6.2.5), and

$$\rho^2 = r^2 + a^2 u^2, \qquad \Delta_u = (1 - u^2)(1 + a^2 u^2) + \frac{2N}{u^{D-5}}. \tag{6.3.2}$$

Our notation and choice of parametrization is different than in [59], but more adequate for our purposes. If we set the NUT parameter[4] $N = 0$ and redefine $u = \cos\theta$ we recover

---

[3]Away from the critical solution, this could be a non-trivial bundle. This will not be important in our analysis.

[4]In the four-dimensional solution, the usual NUT parameter is not exactly the same as N here. The relation is nevertheless easily found.

(6.2.1). Note that having $N \neq 0$ in $D \geq 6$ prevents u from reaching zero, since the last term in Δ_u would blow up.

We are interested in solutions with a single temperature, so we take the same limit as in appendix A to obtain a generalization of (6.2.13),

$$ds^2 = C\rho_0^2(-\sin^2\chi d\tilde{t}^2 + d\chi^2) + \frac{\rho_0^2}{\Delta_u}du^2$$
$$+ \frac{\Delta_u}{\rho_0^2\Xi^2}\left((r_0^2 + a^2)d\tilde{\phi} - 2Cr_0a\Xi\cos\chi d\tilde{t}\right)^2 + r_0^2u^2 d\Omega_{(D-4)}^2 , \quad (6.3.3)$$

where

$$\rho_0^2 = r_0^2 + a^2 u^2 , \quad (6.3.4)$$

and r_0, C are the same functions of a^2 as in sec. 6.2.2. The only non-trivial dependence of the metric is on u.

There are two parameters, a and N. In sec. 6.2.2 we set $N = 0$ and $0 \leq a^2 \leq \infty$, with the critical phase being reached as $a \to \infty$. Here we extend the solutions into a new parameter range by considering negative values of a^2, specifically

$$-\infty \leq a^2 < -1 \quad (6.3.5)$$

as covered when r_0 varies in[5]

$$\frac{D-5}{D-1} < r_0^2 \leq \frac{D-5}{D-3} . \quad (6.3.6)$$

Note that this implies $0 < r_0^2 < 1$, and also $M_0 < 0$. It is convenient to define

$$\alpha^2 = -a^2 , \qquad \hat{C} = Ca^2 , \quad (6.3.7)$$

so that $\alpha^2, \hat{C} > 0$, and

$$\Sigma(u) = \frac{\rho_0^2}{a^2} = u^2 - \frac{r_0^2}{\alpha^2} , \quad (6.3.8)$$

$$\Upsilon(u) = \frac{\Delta_u}{a^2} = (1 - u^2)(u^2 - \alpha^{-2}) + \frac{2\hat{N}}{u^{D-5}} , \quad (6.3.9)$$

where we have conveniently absorbed a power of α in $\hat{N}$. The metric reads[6]

$$ds^2 = \hat{C}\Sigma(-\sin^2\chi d\tilde{t}^2 + d\chi^2) + \frac{\Sigma}{\Upsilon}du^2$$
$$+ \frac{\Upsilon}{\Sigma\Xi^2}\left((\alpha^2 - r_0^2)d\tilde{\phi} + 2i\hat{C}r_0\alpha\Xi\cos\chi d\tilde{t}\right)^2 + r_0^2u^2 d\Omega_{(D-4)}^2 , \quad (6.3.10)$$

---

[5]This range of a^2 is also obtained with $1 < r_0^2 \leq \infty$, but one can see this is not adequate for obeying the required behavior.

[6]Refs. [60, 61] give the Euclidean version of this solution in a different parametrization that is more elegant but less appropriate for our purposes.

This is a complex metric, with imaginary $g_{\tilde{t}\tilde{\phi}}$, since we are taking the rotation parameter a into imaginary values. We will return to this issue below.

We take u to vary in an interval for which Σ and Υ are both non-negative. The zeroes of Υ, which limit this interval, depend on the NUT parameter $\hat{N}$, which so far has been free. When $\hat{N} = 0$, the range in which Υ is positive is

$$\alpha^{-1} \leq u \leq 1 \qquad (\hat{N} = 0) \tag{6.3.11}$$

(we need only consider $u > 0$). Since for $\alpha < \infty$, u is never zero, we fulfill one of the topological requirements on the merged solution: the S^{D-4} never shrinks to zero size. However, since $\alpha^{-1} > r_0/\alpha$, we have that $\Sigma(u)$, although positive, is never zero and therefore the Lorentzian-$S^2_{\tilde{t},\chi}$ is not contractible. This can be remedied by turning on the parameter $\hat{N}$ and tuning it so that the smallest of the two relevant roots of Υ moves to the value r_0/α; the other will be $u_1 > 1$. Then we take

$$\frac{r_0}{\alpha} \leq u \leq u_1 \,. \tag{6.3.12}$$

Note that since now Σ and Υ both have a simple zero at $u = r_0/\alpha$, the $\tilde{\phi}$ circle has finite size there.

While it is easy to solve for the required value of $\hat{N}$ as a function of α, we are mostly interested in the regime where α is very large, in which we approach the critical solution. Then one finds

$$\hat{N} \approx \frac{1}{D-3}\left(\frac{D-5}{D-3}\right)^{\frac{D-5}{2}}\frac{1}{\alpha^{D-3}}, \qquad \frac{r_0}{\alpha} \approx \sqrt{\frac{D-5}{D-3}}\frac{1}{\alpha}, \qquad u_1 \approx 1 + \hat{N}\,. \tag{6.3.13}$$

Note that $\hat{N} \to 0$ as $\alpha \to \infty$.

With these parameter choices, we obtain a solution in which

- as $\alpha \to \infty$ the metric becomes that of the critical solution (6.2.21) (with $u = \cos\theta$),

- there is a contractible Lorentzian-S^2 and a non-contractible S^{D-4}.

- the constant-$\tilde{t}$ sections of the horizon, where $\sin\chi = 0$, have topology $S^2 \times S^{D-4}$. The S^2 is made of the two disks at $\chi = 0, \pi$, joined along $u = r_0/\alpha$.

Therefore, this one-parameter family of solutions satisfies all the properties that we required at the beginning of the section.

Unfortunately, these geometries have two significant shortcomings. First, they are complex, and then it is unclear whether it is sensible to talk about a horizon. Second, and perhaps worse, when the Lorentzian-$S^2_{\tilde{t},\chi}$ shrinks to zero at $u = r_0/\alpha$, it does not

do so smoothly. Near this point, the $(u, \tilde{t}, \chi)$ part of the geometry behaves (up to constant factors) as

$$(u - r_0/\alpha)(-\sin^2\chi d\tilde{t}^2 + d\chi^2) + du^2 \qquad (6.3.14)$$

which is singular at $u = r_0/\alpha$.[7]

The problem of the Lorentzian metric being complex can be remedied by going to the Euclidean section. However, the trouble then comes back in that it does not seem possible to have a regular, real Euclidean section for the solution *before* the merger. It seems we cannot have the real transition both ways.

We have not found any other way of obeying the topology requirements of the merged solution using the family of metrics (6.3.1) than with these parameter choices. It is unclear whether there may be a more general solution that is better behaved.

6.4 Critical geometries for other topology-changing transitions

In sec. 6.2 we have presented an exact instance of an intersection of horizons that gives a satisfactory account of all the aspects of the pre-merger transition conforming to the analysis of [52]. Thus it seems justified to look for local models for the critical geometries in other horizon-merger transitions that are expected to occur for higher-dimensional black holes. We will see that there exist self-similar cone geometries with the adequate properties for all these transitions.

Black ring pinch. The simplest new critical geometry that we describe corresponds to the transition between a black ring with horizon topology $S^1 \times S^{D-3}$ and a black hole with horizon topology S^{D-2} in $D \geq 6$. In the black hole phase, the horizon geometry develops a pinch along the rotation axis, which grows until it pinches off in the critical solution. Coming from the black ring side, the ring becomes fatter until its central hole closes up. The pinch-off occurs on the rotation axis, so we can expect that asymptotically close to this point the rotation is negligible. Thus, the self-similar geometry around this point will be locally a static cone.

In the black ring phase the Euclidean time circle fibers over disks D_2 that fill the ring's hole, to form a S^3. In addition, on the horizon we can find spheres S^{D-4} that shrink to zero size at the inner rim of the ring. Instead, in the black hole phase these S^{D-4} do not shrink anywhere in the region close to the axis, while the previously described S^3 does shrink to zero there. Hence, we have an instance of a conifold-type

---

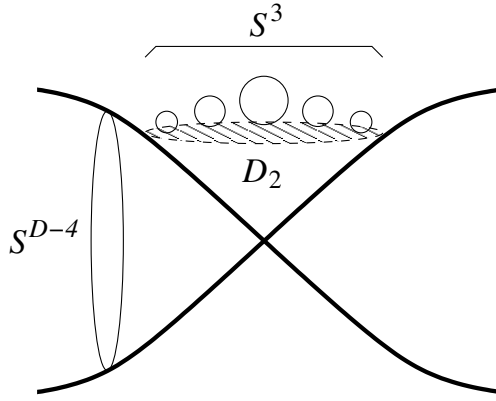[7]The fact that these solutions have $M < 0$ might be behind this.

Figure 6.5: Critical geometry at the 'black ring pinch' transition between a black ring and a topologically spherical black hole. Relative to fig. 4.1, the main difference is that the dashed segment is replaced by a disk D_2. In general, for a p-sphere pinch, the disk D_2 is replaced by a ball B_{p+1}, and the S^3 by a S^{p+2} ($p = 0$ is the case in fig. 4.1).

transition, with the critical geometry being a cone over $S^3 \times S^{D-4}$,

$$ds^2 = dz^2 + \frac{z^2}{D-2}\left(2d\Omega_{(3)}^2 + (D-5)d\Omega_{(D-4)}^2\right) \tag{6.4.1}$$

(see fig. 6.5; this can be obtained by rotating the critical solution of fig. 4.1 around a vertical axis.). The Lorentzian version of the geometry is

$$ds^2 = dz^2 + \frac{2z^2}{D-2}\left(-\cos^2\chi dt^2 + d\chi^2 + \sin^2\chi d\phi^2 + \frac{D-5}{2}d\Omega_{(D-4)}^2\right) \tag{6.4.2}$$

with the horizon being at $\chi = \pi/2$.

Note that this conifold transition can not occur for five-dimensional black rings since the required cone does not exist.

p-sphere pinch. Refs. [28, 29] generalized black rings with horizon $S^1 \times S^{D-3}$ to solutions with horizon $S^p \times S^{D-p-2}$, with odd p, where the S^p is a contractible cycle — we refer to it as an 'odd-sphere blackfold'. Like in a black ring, the S^p has to rotate in order to maintain its equilibrium at a given radius. The approximate method used in [28, 29] is only valid as long as the blackfold is thin, *i.e.,* the S^p is much larger than the S^{D-p-2}, but it is natural to expect that when the angular momentum decreases, the sphere S^p shrinks until its inner hole closes up, like in the example of the black ring. At that point the configuration makes a transition to a topologically-spherical black hole.

In this case the inner hole is a ball B_{p+1} over which the Euclidean time circle fibers, shrinking to zero at the boundary of the ball: this is a S^{p+2}. The size of this sphere

56

remains finite in the odd-sphere-blackfold phase, and shrinks to zero at the axis in the topologically-spherical black hole phase. On the other hand the horizon has a S^{D-p-3} that shrinks to zero size in the odd-sphere blackfold phase, and remains finite (near the axis) in the black hole phase. Thus we have another conifold transition, this time with a critical geometry

$$ds^2 = dz^2 + \frac{p+1}{D-2}z^2\left(d\Omega_{(p+2)}^2 + \frac{D-p-4}{p+1}d\Omega_{(D-p-3)}^2\right),\qquad(6.4.3)$$

and in the Lorentzian version

$$ds^2 = dz^2 + \frac{p+1}{D-2}z^2\left(-\cos^2\chi dt^2 + d\chi^2 + \sin^2\chi d\Omega_{(p)}^2 + \frac{D-p-4}{p+1}d\Omega_{(D-p-3)}^2\right)$$
$$(6.4.4)$$

with $0 \leq \chi \leq \pi/2$ and horizon at $\chi = \pi/2$.

Note that the boundary of B_{p+1} is connected when $p > 0$ so, unlike in sec. 6.2 (which was locally the case $p = 0$ smeared along a circle), in these cases the merger necessarily involves only one horizon.

In the odd-sphere blackfold, when the angular momenta are not all equal, the S^p is not geometrically round. One may reduce some of the angular momenta while the others are kept fixed. In this case we expect a transition to an ultraspinning topologically spherical black hole, controlled by a local geometry of the type above with a collapsing sphere of lower dimensionality.

Circular pinch. Finally, we describe another type of critical pinch-off geometry that is expected to occur in the phase space of higher-dimensional rotating black holes. This is the case of a circular pinch at finite radius on the plane of rotation. This mediates the transition between, for instance, a black Saturn in $D \geq 6$ and a topologically spherical black hole with a circular pinch. The same local critical geometry also appears when two black rings in $D \geq 6$ merge.

The two black objects that merge are rotating, but as they approach we can go to a reference frame that is asymptotically corotating with the two horizons, and in this frame the geometry near the pinch-off point looks again static. This is then locally like in fig. 4.1, spread over the direction of the circle where the horizons touch. The local model for the critical geometry is the same as (6.2.22). Note again that this cannot occur in five dimensions.

It is actually possible to consider also intersecting geometries in which the two black objects have different temperatures, as in (6.2.10), where the horizons touch on a cone but cannot merge. What does not seem possible is to have the two horizons touch over a cone if they have relative non-zero velocity. Presumably, an attempt to force two such horizons to touch gives a stronger singularity.

Given these examples, it is straightforward to extend them to cones for many other transitions that are expected to occur for higher-dimensional black holes.

6.5   Concluding remarks

The main features of the phase space of neutral, asymptotically flat, higher-dimensional black holes are controlled by solutions in three different regions:

(i) Large angular momenta.

(ii) Bifurcations in phase space.

(iii) Topology-changing transitions.

The regime (i) is captured by the blackfold effective theory [28, 27]. Regions (ii) are controlled by zero-mode perturbations of black holes that give rise to bifurcations into new families of solutions. The initial conjectures about these points [56, 45] have been confirmed and extended in [62]. In this chapter we have begun to explore regions (iii) in $D \geq 6$ and provided local models for the critical geometries that effect the topology change.

We have presented an example where we can study in a detailed exact manner the geometry in a topology-changing transition, at least in one of the sides of the transition and at the critical point itself. The critical geometry conforms precisely to the predictions of [52]. It seems valuable to have an exact and simple analytic model of one such transition from which one can extract further details. In particular, a more detailed study of how the conical geometries, including the large class of examples in appendix B, are resolved away from the critical point is probably of interest.

We have also seen that self-similar cone geometries occur when two horizons intersect but cannot merge since their temperatures are unequal. In this case the cone is over a warped product, not a direct one, and the arguments of [52] would not apply. Nevertheless, the extension we have found is a natural one: the direct-product Nariai solution at the base of the cone is simply replaced by the more general Schwarzschild-deSitter solution. This allows to study intersecting horizons in more generality.

Topology-changing transitions among five-dimensional asymptotically flat rotating black holes do not fall within the class studied in this chapter. Indeed, the phase diagram of five-dimensional black holes, say with a single spin, already reveals that the transitions are controlled by a different class of critical geometry, not of the conifold type. The same is true of transitions that are effectively in that same class by

having some directions smeared along the intersection (*e.g.,* black Saturn or black di-ring mergers), and in general those that involve a collapsing S^1. The study of these transitions deserves a separate investigation.

Chapter 7

Summary of results

- In chapter 5 we managed to formulate a type of fluid-gravity correspondence for asymptotically flat black branes. We found a map between a fluctuating boosted black $p-$brane and a relativistic viscous fluid living at spatial infinity. That is, we constructed a solution to the vacuum Einstein equations of a dynamical black $p-$brane up to first order in derivatives. The dual viscous fluid is characterized by two parameters (transport coefficients) in the stress tensor $-$ the shear and bulk viscosities. Using the gravitational solution we succeeded to compute those coefficients. Namely, we found that the fluid stress tensor is

$$T_{ab} = \rho u_a u_b + P P_{ab} - \zeta \theta P_{ab} - 2\eta \sigma_{ab} + O(\partial^2) \tag{7.0.1}$$

  where

$$\eta = \frac{\Omega_{n+1}}{16\pi G} r_0^{n+1}, \qquad \zeta = \frac{\Omega_{n+1}}{8\pi G} r_0^{n+1} \left(\frac{1}{p} + \frac{1}{n+1} \right). \tag{7.0.2}$$

  are the shear and bulk viscosities, respectively. For more details on the notations and on what each quantity in the stress tensor is see chapter 5 . Furthermore, by using the effective description of the black $p-$brane as a viscous fluid in a lower number of dimensions we studied the Gregory-Laflamme instability and we found a striking agreement with the numerical results, already obtained, on this problem (those are gravitational calculations). Hence, instead of attacking the complicated (linearized) gravitational equations we propose instead to attack the relativistic Navier-Stokes equations of the effective (dual) fluid, as they are much simpler than the former.

- In chapter 6 we tackled and made progress in a different problem $-$ topology change in higher dimensional general relativity. Before our work there had been no analytical (but only numerical) complete example of a topological phase transition in general relativity. The black string / black hole phase transition in

Kaluza-Klein spaces was analyzed and studied only numerically. Neverthelss, some local models had been obtained analytically. It was argued that the phase transition passes through (or is mediated by) a singular critical configurtaion; a self-similar double cone geometry. This geometry was found **only locally**, though. In our work we have provided for the first time a complete analytical example of a topological phase transition (it has some shortcomings, though, see chapter 6). We took the rotating black hole inside de-Sitter space (the Kerr-de-Sitter black hole), and we showed that if one follows a trajectory in the phase space of solutions along which the black hole rotation is increased then it will pancake along the rotation plane, and finally it will touch the de-Sitter horizon along that plane. A merger transition is obtained if one continues to move along the same phase space trajectory, leading to a merged phase with a single connected horizon. In our example, the critical configuration (in which the two horizons just meet) is mediated by a self-similar double cone, thus confirming previous propositions of the mechanism under which topological transitions work.

We also described local models for the critical geometries that control many transitions in the phase space of higher-dimensional black holes, such as the pinch-down of a topologically spherical black hole to a black ring or to a black p-sphere, or the merger between black holes and black rings in black Saturns or di-rings in $D \geq 6$.

It is worth mentioning, in addition, that the cones we have found are general ones (compared to previousely known ones), in the sense that they descibe two horizons that intersect each other at different temperatures, not only ones that intersect each other with the same temperature. However, in the case the two horizons intersect at different temperatures, there can be no merger transition afterwards, and so the trajectory of solutions in the phase space ends there.

Appendix A

Equal-temperature limit

In this appendix we define a limit of the Kerr-deSitter solutions (6.2.1) and the Kerr-NUT-deSitter solutions (6.3.1) that generalizes the well-known Nariai limit of the Schw-dS solution[1]. We use units where the cosmological radius is $L = 1$.

In order for the two horizons of (6.2.1) to have equal surface gravities, or equal temperatures, the value of the radial coordinate r must be the same for both, $i.e.$, Δ_r must have a double root $r = r_0$,

$$\Delta_r(r_0) = \partial_r \Delta_r(r_0) = 0 \,. \tag{A.0.1}$$

These two conditions determine the values of M and a as functions of r_0,

$$M_0 = r_0^{D-3}\frac{(1-r_0^2)^2}{(D-3)r_0^2-(D-5)} \,, \qquad a^2 = r_0^2\frac{D-3-(D-1)r_0^2}{(D-3)r_0^2-(D-5)} \,. \tag{A.0.2}$$

Although their radial coordinates coincide, the proper radial distance between the two horizons goes to a finite non-zero limit. We can pry open the space between them by first introducing a small parameter ε that takes us slightly away from the limit, with a new 'radial' coordinate χ,

$$r = r_0(1 - \varepsilon \cos \chi) \,, \tag{A.0.3}$$

and

$$M = M_0 \left(1 - \frac{r_0^2}{C(r_0^2 + a^2)(1 - r_0^2)}\varepsilon^2 \right) \,, \tag{A.0.4}$$

where C is as in (6.2.17). Then redefine appropriately the Killing coordinates t and ϕ to

$$t = C\frac{r_0^2 + a^2}{r_0}\frac{\tilde{t}}{\varepsilon} \,, \qquad \phi = \tilde{\phi} + C\frac{a(1 - r_0^2)}{r_0}\frac{\tilde{t}}{\varepsilon} \,. \tag{A.0.5}$$

Finally, take the limit $\varepsilon \to 0$ to find the finite metric (6.2.13).

---

[1] Ref. [63] describes essentially the same limit, but in a different parametrization.

The limit fixes one of the two dimensionless free parameters of the original solution, leaving r_0, or a, as the only parameter. In this work we are interested in approaching the solutions that satisfy (6.2.7), (6.2.8). In the one-parameter family, this corresponds to

$$r_0^2 \to \frac{D-5}{D-3} \,. \tag{A.0.6}$$

Indeed in this limit

$$a \to \infty \,, \qquad M_0 \to \infty \,, \tag{A.0.7}$$

while

$$\frac{M_0}{a^2} \to \frac{1}{D-5} \left(\frac{D-5}{D-3} \right)^{\frac{D-3}{2}} \tag{A.0.8}$$

remains finite. Also, in this limit $Ca^2 \to 1/(D-3)$.

Appendix B

General black hole-deSitter intersections

Here we extend the analysis of sec. 6.2 to the situation where the black hole rotates in an arbitrary number of planes. The starting solution is the general Kerr-deSitter metric as given in ref. [64], whose presentation we follow closely.

In order to have a unified description for even and odd D, we introduce

$$\epsilon = (D - 1) \bmod 2 \,. \tag{B.0.1}$$

The spacetime dimension is then $D = 2n + \epsilon + 1$, where n is the number of orthogonal rotation planes. On each of these, we choose angles ϕ_i with period 2π. We also introduce an overall radial coordinate r and $n + \epsilon$ direction cosines μ_i satisfying

$$\sum_{i=1}^{n+\epsilon} \mu_i^2 = 1 \,, \tag{B.0.2}$$

with $0 \leq \mu_i \leq 1$, $i = 1, \ldots, n$. In even D the μ_{n+1} has range $-1 \leq \mu_{n+1} \leq 1$.

The solution is characterized by a mass parameter M and n rotation parameters a_i, and its metric is

$$ds^2 = -W\left(1 - \frac{r^2}{L^2}\right)dt^2 + \frac{2M}{U}\left(W\,dt - \sum_{i=1}^{n} \frac{a_i\,\mu_i^2}{1 + \frac{a_i^2}{L^2}}\,d\phi_i\right)^2 + \sum_{i=1}^{n} \frac{r^2 + a_i^2}{1 + \frac{a_i^2}{L^2}}\,\mu_i^2\,d\phi_i^2$$

$$+ \frac{U}{V - 2M}dr^2 + \sum_{i=1}^{n+\epsilon} \frac{r^2 + a_i^2}{1 + \frac{a_i^2}{L^2}}d\mu_i^2 + \frac{1}{W(L^2 - r^2)}\left(\sum_{i=1}^{n+\epsilon} \frac{(r^2 + a_i^2)\,\mu_i\,d\mu_i}{1 + \frac{a_i^2}{L^2}}\right)^2 \tag{B.0.3}$$

where

$$U = r^\epsilon \sum_{i=1}^{n+\epsilon} \frac{\mu_i^2}{r^2 + a_i^2} \prod_{l=1}^{n}(r^2 + a_l^2) \,, \tag{B.0.4}$$

65

$$V = r^{\epsilon-2} \left(1 - \frac{r^2}{L^2}\right) \prod_{i=1}^{n} (r^2 + a_i^2) \,, \tag{B.0.5}$$

and

$$W = \sum_{i=1}^{n+\epsilon} \frac{\mu_i^2}{1 + \frac{a_i^2}{L^2}} \,. \tag{B.0.6}$$

We take the limit in which we send a number s of rotation parameters to infinity, all at the same rate. For now, the remaining $n - s$ ones are set to zero, so

$$
\begin{aligned}
a_j &\to \infty \,, & j &= 1, \ldots, s \,, \\
a_k &= 0 \,, & k &= s+1, \ldots, n \,,
\end{aligned}
\tag{B.0.7}
$$

with

$$2s \leq D - 4 \,. \tag{B.0.8}$$

At the same time we send $M \to \infty$ in such a way that

$$\mu = \frac{2M}{\prod_{j=1}^{s} a_j^2} \tag{B.0.9}$$

remains finite (compare to appendix A of [56]).

We introduce an angular variable θ such that

$$\sum_{j=1}^{s} \mu_j^2 = \sin^2 \theta \,, \qquad \sum_{k=s+1}^{n+\epsilon} \mu_k^2 = \cos^2 \theta \,, \tag{B.0.10}$$

with range $0 \leq \theta \leq \pi/2$. With this variable, the metric on the unit S^{D-2} is written as

$$\sum_{i=1}^{n+\epsilon} d\mu_i^2 + \sum_{i=1}^{n} \mu_i^2 d\phi_i^2 = d\Omega^2_{(D-2)} = d\theta^2 + \sin^2 \theta \, d\Omega^2_{(2s-1)} + \cos^2 \theta \, d\Omega^2_{(D-2s-2)} \,. \tag{B.0.11}$$

After some labor one finds the limiting geometry

$$ds^2 = L^2 \left(d\theta^2 + \sin^2 \theta d\Omega^2_{(2s-1)}\right) + \cos^2 \theta \left(-f(r)dt^2 + \frac{dr^2}{f(r)} + r^2 d\Omega^2_{(D-2s-2)}\right) \tag{B.0.12}$$

with

$$f(r) = 1 - \frac{\mu}{r^{D-2s-3}} - \frac{r^2}{L^2} \,. \tag{B.0.13}$$

Near $\theta = \pi/2$ this has the form of a cone over Schw-dS$_{D-2s}$, spread over a sphere S^{2s-1}. When $s = 1$ we recover (6.2.9). The restriction (B.0.8) on the number s of 'ultraspins' guarantees that the Schw-dS$_{D-2s}$ factor in the limit geometry is at least four-dimensional.

It is easy to generalize the limit to

$$a_j \to \infty, \qquad j = 1, \ldots, s,$$
$$a_k \ \text{finite}, \qquad k = s+1, \ldots, n, \tag{B.0.14}$$

again with finite μ in (B.0.9) to obtain the geometry

$$ds^2 = L^2 \left(d\theta^2 + \sin^2\theta \, d\Omega^2_{(2s-1)}\right) + \cos^2\theta \, ds^2 \left(\text{Kerr-dS}_{(D-2s)}\right), \tag{B.0.15}$$

where Kerr-dS$_{(D-2s)}$ has the finite a_k as rotation parameters. The Euclidean version of the latter solution is known to contain many interesting Einstein metrics, in addition to products $S^2 \times S^{D-2s-2}$, such as Page's metric for the non-trivial S^2 bundle over S^2 [65] and higher-dimensional generalizations thereof (see *e.g.*, [60] and references to it). Our construction results in cones over all these spaces. It may be interesting to study them in more detail.

Bibliography

[1] C. W. Misner, K. S. Thorne and J. A. Wheeler, "Gravitation", (1973) San Francisco.

[2] S. Weinberg, "Gravitation and cosmology", (1972), John Wiley and Sons, Inc.

[3] R. M. Wald, "General Relativity", (1984), University of Chicago.

[4] J. D. Bekenstein, "Black Holes and Entropy", Phys. Rev. D 7, 2333-2346 (1973).

[5] S .W. Hawking, "Particle creation by black holes", Comm. Math. Phys. Volume 43, Number 3 (1975), 199-220.

[6] N. D. Birrell and P. C. W. Davies, "Quantum Fields In Curved Space", Cambridge University Press, 1982.

[7] G. 't Hooft, "Dimensional reduction in quantum gravity," gr-qc/9310026.

[8] L. Susskind, "The World as a hologram," J. Math. Phys. **36** (1995) 6377 [hep-th/9409089].

[9] S. W. Hawking and G. F. R. Ellis, "The Large Scale Structure of Space-Time", Cambridge University Press, 1973.

[10] K. Becker, M. Becker and J. H. Schwarz, "STRING THEORY AND M-THEORY", Cambridge University Press, 2007.

[11] J. Polchinski, "String Theory" in two volumes. Cambridge: Cambridge University Press 1998.

[12] A. Strominger and C. Vafa, "Microscopic origin of the Bekenstein-Hawking entropy," Phys. Lett. B **379** (1996) 99 [hep-th/9601029].

[13] R. C. Myers and M. J. Perry, "Black Holes In Higher Dimensional Space-Times," Annals Phys. 172, 304 (1986).

[14] R. Emparan and H. S. Reall, "Black Rings," Class. Quant. Grav. **23** (2006) R169 [hep-th/0608012].

[15] H. Elvang and P. Figueras, "Black Saturn," JHEP 0705 (2007) 050 [arXiv:hep-th/0701035].

[16] H. Iguchi and T. Mishima, "Black di-ring and infinite nonuniqueness," Phys. Rev. D **75** (2007) 064018 [Erratum-ibid. D **78** (2008) 069903] [hep-th/0701043].

[17] J. M. Maldacena, "The Large N limit of superconformal field theories and supergravity," Adv. Theor. Math. Phys. **2** (1998) 231 [hep-th/9711200].

[18] O. Aharony, S. S. Gubser, J. M. Maldacena, H. Ooguri and Y. Oz, "Large N field theories, string theory and gravity," Phys. Rept. **323** (2000) 183 [hep-th/9905111].

[19] J. Maldacena, "The Gauge/gravity duality," arXiv:1106.6073 [hep-th].

[20] J. Polchinski, "Dirichlet Branes and Ramond-Ramond charges," Phys. Rev. Lett. **75** (1995) 4724 [hep-th/9510017].

[21] V. E. Hubeny, S. Minwalla and M. Rangamani, "The fluid/gravity correspondence," arXiv:1107.5780 [hep-th].

[22] G. Policastro, D. T. Son and A. O. Starinets, "The Shear viscosity of strongly coupled N=4 supersymmetric Yang-Mills plasma," Phys. Rev. Lett. **87** (2001) 081601 [hep-th/0104066].

[23] E. Witten, "Quantum gravity in de Sitter space," hep-th/0106109.

[24] A. Strominger, "The dS / CFT correspondence," JHEP **0110** (2001) 034 [hep-th/0106113].

[25] T. Damour, "Surface Effects in Black Hole Physics", Proceedings of the Second Marcel Grossmann Meeting on General Relativity, (edited by R. Ruffini, North Holland, 1982) p. 587.

K. S. Thorne, R. H. Price and D. A. Macdonald, *"Black Holes: The Membrane Paradigm"*, Yale Univ. Press, New Haven, USA (1986).

[26] S. Bhattacharyya, V. E. Hubeny, S. Minwalla and M. Rangamani, "Nonlinear Fluid Dynamics from Gravity," JHEP **0802** (2008) 045 [arXiv:0712.2456 [hep-th]].

[27] R. Emparan, T. Harmark, V. Niarchos and N. A. Obers, "Essentials of Blackfold Dynamics," JHEP **1003** (2010) 063 [arXiv:0910.1601 [hep-th]].

[28] R. Emparan, T. Harmark, V. Niarchos and N. A. Obers, "Worldvolume Effective Theory for Higher-Dimensional Black Holes (Blackfolds)," Phys. Rev. Lett. **102**, 191301 (2009) [arXiv:0902.0427 [hep-th]].

[29] R. Emparan, T. Harmark, V. Niarchos and N. A. Obers, "New Horizons for Black Holes and Branes," arXiv:0912.2352 [hep-th].

[30] P. Kovtun, D. T. Son and A. O. Starinets, "Viscosity in strongly interacting quantum field theories from black hole physics," Phys. Rev. Lett. **94** (2005) 111601 [arXiv:hep-th/0405231].

[31] A. Buchel, "Bulk viscosity of gauge theory plasma at strong coupling," Phys. Lett. B **663**, 286 (2008) [arXiv:0708.3459 [hep-th]].

[32] N. Iqbal and H. Liu, "Universality of the hydrodynamic limit in AdS/CFT and the membrane paradigm," Phys. Rev. D **79** (2009) 025023 [arXiv:0809.3808 [hep-th]].

[33] M. Fujita, "Non-equilibrium thermodynamics near the horizon and holography," JHEP **0810** (2008) 031 [arXiv:0712.2289 [hep-th]].

[34] R. Gregory and R. Laflamme, "Black strings and p-branes are unstable," Phys. Rev. Lett. **70** (1993) 2837 [arXiv:hep-th/9301052]; "The Instability of charged black strings and p-branes," Nucl. Phys. B **428** (1994) 399 [arXiv:hep-th/9404071].

[35] A. Buchel, "A holographic perspective on Gubser-Mitra conjecture," Nucl. Phys. B **731** (2005) 109 [arXiv:hep-th/0507275].

[36] J. D. Brown and J. W. York, "Quasilocal energy and conserved charges derived from the gravitational action," Phys. Rev. D **47** (1993) 1407 [arXiv:gr-qc/9209012].

[37] A. Ashtekar and J. D. Romano, "Spatial infinity as a boundary of space-time," Class. Quant. Grav. **9** (1992) 1069.

[38] D. Marolf, "Asymptotic flatness, little string theory, and holography," JHEP **0703**, 122 (2007) [arXiv:hep-th/0612012].

[39] M. M. Caldarelli, O. J. C. Dias, R. Emparan and D. Klemm, "Black Holes as Lumps of Fluid," JHEP **0904** (2009) 024 [arXiv:0811.2381 [hep-th]].

[40] B. Kol and E. Sorkin, "On black-brane instability in an arbitrary dimension," Class. Quant. Grav. **21** (2004) 4793 [arXiv:gr-qc/0407058].

[41] V. Asnin, D. Gorbonos, S. Hadar, B. Kol, M. Levi and U. Miyamoto, "High and Low Dimensions in The Black Hole Negative Mode," Class. Quant. Grav. **24** (2007) 5527 [arXiv:0706.1555 [hep-th]].

[42] V. Cardoso and O. J. C. Dias, "Gregory-Laflamme and Rayleigh-Plateau instabilities," Phys. Rev. Lett. **96**, 181601 (2006) [arXiv:hep-th/0602017].

[43] K. i. Maeda and U. Miyamoto, "Black hole-black string phase transitions from hydrodynamics," JHEP **0903**, 066 (2009) [arXiv:0811.2305 [hep-th]].

[44] O. Aharony, S. Minwalla and T. Wiseman, "Plasma-balls in large N gauge theories and localized black holes," Class. Quant. Grav. **23** (2006) 2171 [arXiv:hep-th/0507219].

[45] R. Emparan, T. Harmark, V. Niarchos, N. A. Obers and M. J. Rodriguez, "The Phase Structure of Higher-Dimensional Black Rings and Black Holes," JHEP **0710** (2007) 110 [arXiv:0708.2181 [hep-th]].

[46] M. M. Caldarelli, R. Emparan and M. J. Rodriguez, "Black Rings in (Anti)-deSitter space," JHEP **0811**, 011 (2008) [arXiv:0806.1954 [hep-th]].

[47] S. Bhattacharyya, R. Loganayagam, S. Minwalla, S. Nampuri, S. P. Trivedi and S. R. Wadia, "Forced Fluid Dynamics from Gravity," JHEP **0902** (2009) 018 [arXiv:0806.0006 [hep-th]].

[48] B. Kol, "The Phase transition between caged black holes and black strings: A Review," Phys. Rept. **422** (2006) 119-165. [hep-th/0411240].

T. Harmark, N. A. Obers, "Phases of Kaluza-Klein black holes: A Brief review," [hep-th/0503020].

G. T. Horowitz, T. Wiseman, "General black holes in Kaluza-Klein theory," [arXiv:1107.5563 [gr-qc]].

[49] S. S. Gubser, "On nonuniform black branes," Class. Quant. Grav. **19** (2002) 4825-4844. [hep-th/0110193].

T. Wiseman, "Static axisymmetric vacuum solutions and nonuniform black strings," Class. Quant. Grav. **20** (2003) 1137-1176. [hep-th/0209051].

B. Kleihaus, J. Kunz, E. Radu, "New nonuniform black string solutions," JHEP **0606** (2006) 016. [hep-th/0603119].

E. Sorkin, "Non-uniform black strings in various dimensions," Phys. Rev. **D74** (2006) 104027. [gr-qc/0608115].

[50] T. Harmark, N. A. Obers, "Black holes on cylinders," JHEP **0205** (2002) 032. [hep-th/0204047].

T. Wiseman, "From black strings to black holes," Class. Quant. Grav. **20** (2003) 1177-1186. [hep-th/0211028].

B. Kol, E. Sorkin, T. Piran, "Caged black holes: Black holes in compactified space-times. 1. Theory," Phys. Rev. **D69** (2004) 064031. [hep-th/0309190].

E. Sorkin, B. Kol, T. Piran, "Caged black holes: Black holes in compactified space-times. 2. 5-d numerical implementation," Phys. Rev. **D69** (2004) 064032. [hep-th/0310096].

T. Harmark, N. A. Obers, "Phase structure of black holes and strings on cylinders," Nucl. Phys. **B684** (2004) 183-208. [hep-th/0309230].

H. Kudoh, T. Wiseman, "Properties of Kaluza-Klein black holes," Prog. Theor. Phys. **111** (2004) 475-507. [hep-th/0310104].

H. Kudoh, T. Wiseman, "Connecting black holes and black strings," Phys. Rev. Lett. **94** (2005) 161102. [hep-th/0409111].

[51] M. Headrick, S. Kitchen, T. Wiseman, "A New approach to static numerical relativity, and its application to Kaluza-Klein black holes," Class. Quant. Grav. **27** (2010) 035002. [arXiv:0905.1822 [gr-qc]].

[52] B. Kol " Topology change in General Relativity, and the black-hole black-string transition," JHEP **10** (2005) 049 [arXiv:hep-th/0206220].

[53] B. Kol, T. Wiseman " Evidence that highly non-uniform black strings have a conical waist," Class. Quant. Grav. **20** (2003) 3493 [arXiv:hep-th/0304070v2].

[54] V. Asnin, B. Kol, M. Smolkin, "Analytic evidence for continuous self similarity of the critical merger solution," Class. Quant. Grav. **23** (2006) 6805-6827. [hep-th/0607129].

[55] R. Emparan, P. Figueras, "Multi-black rings and the phase diagram of higher-dimensional black holes," JHEP **1011** (2010) 022. [arXiv:1008.3243 [hep-th]].

[56] R. Emparan, R. C. Myers, "Instability of ultra-spinning black holes," JHEP **0309** (2003) 025. [arXiv:hep-th/0308056 [hep-th]].

[57] L. Lehner, F. Pretorius, "Black Strings, Low Viscosity Fluids, and Violation of Cosmic Censorship," Phys. Rev. Lett. **105** (2010) 101102. [arXiv:1006.5960 [hep-th]].

[58] S. W. Hawking, C. J. Hunter, M. Taylor, "Rotation and the AdS / CFT correspondence," Phys. Rev. **D59** (1999) 064005. [hep-th/9811056].

[59] D. Klemm, "Rotating black branes wrapped on Einstein spaces," JHEP **9811** (1998) 019. [hep-th/9811126].

[60] H. Lu, D. N. Page, C. N. Pope, "New inhomogeneous Einstein metrics on sphere bundles over Einstein-Kahler manifolds," Phys. Lett. **B593** (2004) 218-226. [hep-th/0403079].

[61] R. B. Mann, C. Stelea, "New multiply nutty spacetimes," Phys. Lett. **B634** (2006) 448-455. [hep-th/0508203].

[62] O. J. C. Dias, P. Figueras, R. Monteiro, J. E. Santos, R. Emparan, "Instability and new phases of higher-dimensional rotating black holes," Phys. Rev. **D80** (2009) 111701. [arXiv:0907.2248 [hep-th]].

O. J. C. Dias, P. Figueras, R. Monteiro, J. E. Santos, "Ultraspinning instability of rotating black holes," Phys. Rev. **D82** (2010) 104025. [arXiv:1006.1904 [hep-th]].

M. Durkee, H. S. Reall, "Perturbations of near-horizon geometries and instabilities of Myers-Perry black holes," Phys. Rev. **D83** (2011) 104044. [arXiv:1012.4805 [hep-th]].

O. J. C. Dias, R. Monteiro, J. E. Santos, "Ultraspinning instability: the missing link," JHEP **1108** (2011) 139. [arXiv:1106.4554 [hep-th]].

[63] Z. W. Chong, G. W. Gibbons, H. Lu, C. N. Pope, "Separability and killing tensors in Kerr-Taub-NUT-de sitter metrics in higher dimensions," Phys. Lett. **B609** (2005) 124-132. [hep-th/0405061].

[64] G. W. Gibbons, H. Lu, D. N. Page, C. N. Pope, "Rotating black holes in higher dimensions with a cosmological constant," Phys. Rev. Lett. **93** (2004) 171102. [hep-th/0409155].

[65] D. N. Page, "A Compact Rotating Gravitational Instanton," Phys. Lett. **B79** (1978) 235.

[66] R. Emparan, "Blackfolds," arXiv:1106.2021 [hep-th].

[67] R. Emparan, T. Harmark, V. Niarchos and N. A. Obers, "Blackfolds in Super-gravity and String Theory," JHEP **1108** (2011) 154 [arXiv:1106.4428 [hep-th]].

[68] M. M. Caldarelli, R. Emparan and B. Van Pol, "Higher-dimensional Rotating Charged Black Holes," JHEP **1104** (2011) 013 [arXiv:1012.4517 [hep-th]].

[69] J. Camps and R. Emparan, "Derivation of the blackfold effective theory," JHEP **1203** (2012) 038 [Erratum-ibid. **1206** (2012) 155] [arXiv:1201.3506 [hep-th]].

[70] G. T. Horowitz, T. Wiseman, "General black holes in Kaluza-Klein theory," [arXiv:1107.5563 [gr-qc]].

[71] T. Harmark, N. A. Obers, "Phases of Kaluza-Klein black holes: A Brief review," [hep-th/0503020].

[72] T. Harmark, "Small black holes on cylinders," Phys. Rev. D **69** (2004) 104015 [hep-th/0310259].

[73] D. Gorbonos and B. Kol, "A Dialogue of multipoles: Matched asymptotic expansion for caged black holes," JHEP **0406** (2004) 053 [hep-th/0406002].

[74] H. Kudoh and T. Wiseman, "Connecting black holes and black strings," Phys. Rev. Lett. **94** (2005) 161102 [hep-th/0409111].

[75] H. Kudoh and T. Wiseman, "Properties of Kaluza-Klein black holes," Prog. Theor. Phys. **111** (2004) 475 [hep-th/0310104].